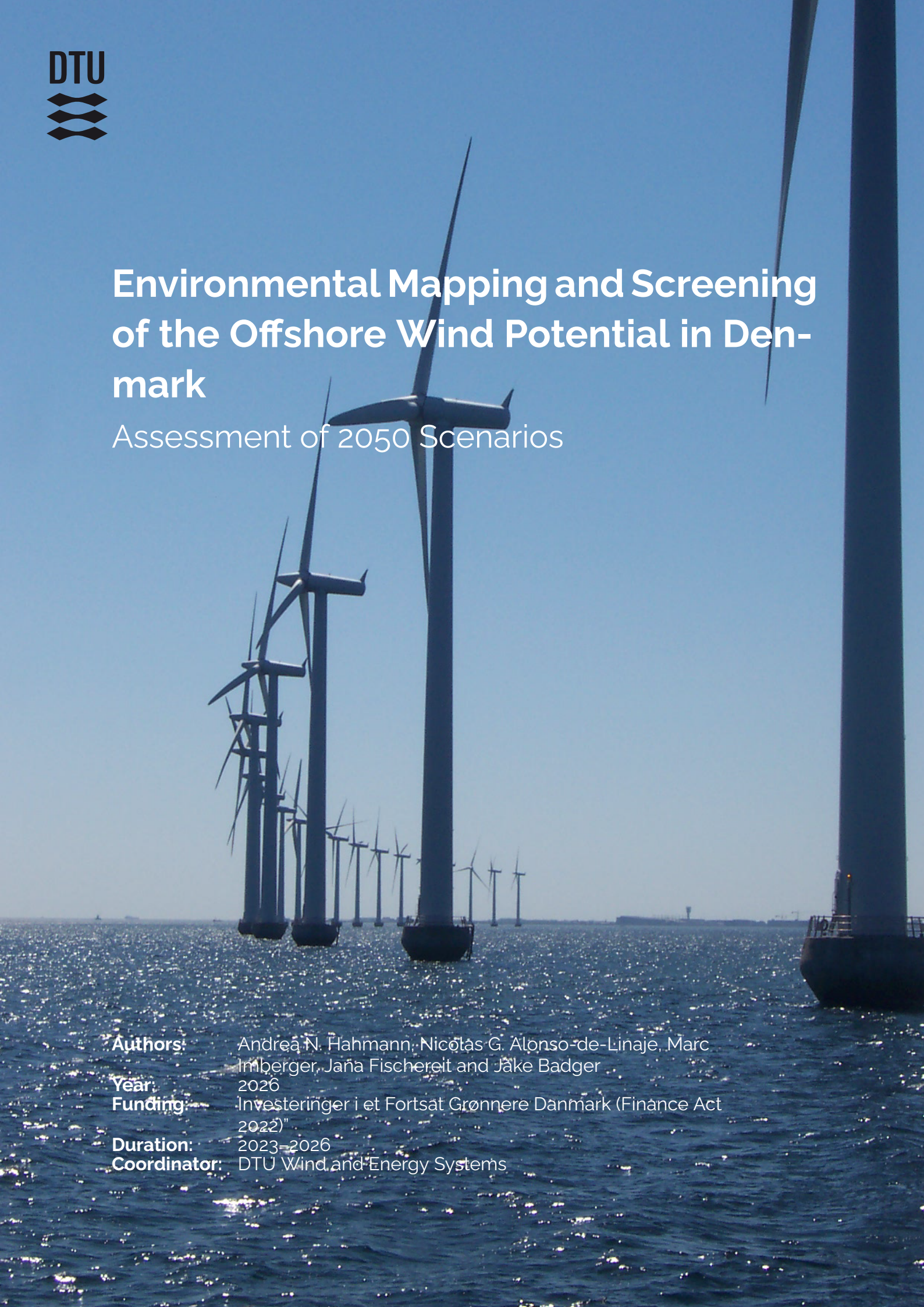
Environmental Mapping and Screening of the Offshore Wind Potential in Denmark

Assessment of 2050 Scenarios



Authors: Andrea N. Hahmann, Nicolas G. Alonso-de-Linaje, Marc Imberger, Jana Fischereit and Jake Badger

Year: 2026
Funding: Investeringer i et Fortsat Grønnere Danmark (Finance Act 2022)"
Duration: 2023–2026
Coordinator: DTU Wind and Energy Systems

Project acronym ENS-DK	Project Title Screening af Havvindpotentialet i Danmark	Project Coordinator NIRAS
Delopgave #1 Følsom-hedskortlægning	Deliverable Title Environmental Mapping and Screening of the Offshore Wind Potential in Denmark	Version Final
Type Report and Data	Dissemination Level Assessment of 2050 Scenarios	Due Date October 26, 2026
Lead Beneficiary DTU Department of Wind and Energy Systems		Pages 37
Lead Author Andrea N. Hahmann (DTU)	Reviewed by Jake Badger	

Disclaimer

This deliverable contains original unpublished work except where clearly indicated otherwise. Acknowledgement of previously published material and of the work of others has been made through appropriate citation, quotation or both. Reproduction is authorized provided the source is acknowledged.

Acknowledgements
The authors further acknowledge support from the Danish Energy Agency under the political sub-agreement to the Finance Act 2022 (Investeringer i et fortsat grønnere Danmark).

History of Changes

Date	Version	Author/Reviewer	Comments
5-12-2025	1.0	Andrea N. Hahmann (DTU)	First draft
12-01-2026	2.0	Andrea N. Hahmann (DTU)	New 2050 scenarios included
25-02-2026	2.1	DEA & Andrea N. Hahmann (DTU)	Second round of comments
01-05-2026	3.0	Andrea N. Hahmann (DTU)	Revised text and data
08-06-2026	3.1	DEA & Andrea N. Hahmann (DTU)	Revised text and figures
01-07-2026	4.0	Andrea N. Hahmann (DTU)	Final version
26-10-2026	Final	Report approved by the DEA	

Executive Summary

Operating large offshore wind farms reduces wind speeds within and downwind of them. This phenomenon, known as wind farm wake, can significantly influence annual energy output, especially in regions with high installed capacity density. To evaluate this in Danish waters, we employ a mesoscale model to simulate atmospheric conditions and the effects of wind farms on them. The results in this report are subject to considerable uncertainty, as many aspects of the modelling outcomes remain unvalidated. Comprehensive data needed to validate the simulations are absent, primarily due to the scarcity of extensive observations, and large wind farms similar to those envisioned for the 2050 scenario have yet to be established.

We model the flow to estimate wind resources for the North Sea, South Baltic Sea, and the Kattegat for a single meteorological year, using several wind farm scenarios: (i) no wind farms, (ii) existing farms as of November 2021, (iii) planned deployment in 2030, and (iv) hypothetical scenarios for 2050, with three different scenarios for offshore wind deployment and the nearly identical total installed capacities. We simulate reductions in average wind speed and other climate variables resulting from the presence of wind farms. We also evaluate reductions in capacity factors, power yields, and full-load hours resulting from changes in wind speed.

The main conclusions of this report can be summarised as follows:

- Large offshore wind farms lower wind speeds within and downwind of clusters. In the 2050 scenario, the Danish EEZ in the North Sea could face wind speed deficits of up to $-2.5\,\mathrm{m\,s^{-1}}$ on average within the large wind farms near the German border, with half the area experiencing reductions of at least $-0.25\,\mathrm{m\,s^{-1}}$.
- The simulations show minor changes in air temperature at 2 meters, a slight increase in boundary layer height, and slight increases in cloud fraction, exclusively near large clusters. These changes are likely not statistically significant at the 95 % level but robust under some atmospheric conditions.
- The 2050 offshore wind scenarios show wake losses of 13–24%, only slightly higher than in 2030 (11–20%), due to larger capacity and clustering. The small increase from 2030 to 2050 results from low capacity densities and wind farm locations in areas with excellent wind resources.
- Despite wake losses, annual energy production increases in future scenarios due to higher capacity and improved siting of offshore wind farms in windier areas. In Denmark, for a typical year of 2019, turbines under the CURRENT scenario yield about ∼24 TWh, increasing to 84–94 TWh by 2030 and 210–240 TWh by 2050.
- The scenario with many small, dense wind farms best balances the reduction of wake effects and the increase in energy output, despite potentially higher costs. This setup spreads installed capacity across multiple smaller sites throughout the Danish North Sea, thereby utilising windier regions, minimising internal wakes, and enabling better replenishment between wind farms.
- With ample space and excellent wind conditions, many scenarios can achieve 35 GW of offshore wind capacity in the Danish North Sea, maximising power output. Both large, low-capacity-density farms and smaller farms help reduce wake effects, making either option feasible.

Abbreviations

Acronym	Description
AGL	Above ground level
DEA	Danish Energy Agency
EEZ	Exclusive Economic Zone
EWP	Explicit Wake Parameterization
FITCH	Fitch et al. wind farm parameterisation
FLH	Full load hours
IC	Installed capacity
WFP	Wind farm parameterisation
WRF	Weather, Research and Forecasting (model)

Contents

History of Changes . . . 2

Executive Summary . . . 3

1 Preface . . . 6

2 Introduction . . . 7

3 Mesoscale and wind farm model . . . 8
3.1 The Large domain . . . 8
3.2 The Small Danish domain . . . 10

4 Results . . . 13
4.1 The Large domain . . . 13
4.2 The Small Danish domain . . . 22
4.3 Comparison of the Large and Small Danish domains . . . 28

5 Summary and conclusions . . . 30

References . . . 31

ANNEXES . . . 33
Annex 1 Analysis for the whole domain . . . 33

1 Preface

This report contributes to the project "Environmental mapping and screening of sites for offshore wind in Denmark, " initiated in 2022 by the Danish Energy Agency. The project aims to support the long-term planning of offshore wind farms by providing a comprehensive overview of the combined offshore wind potential in Denmark. It is funded under the Finance Act 2022 through the programme "Investeringer i et fortsat grønnere Danmark" (Investing in the continuing greening of Denmark). The project is carried out by NIRAS, Aarhus University (Department of Ecoscience) and DTU (Department of Wind and Energy Systems).

The overall project consists of four tasks defined by the Danish Energy Agency (https://ens.dk/ansvarsomraader/vindmoeller-paa-hav/planlaegning-af-fremtidens-havvindmoelleparker):

- Sensitivity mapping of nature, environmental, wind and hydrodynamic conditions.
- Technical fine-screening and assessment of the overall offshore wind potential based on the sensitivity mapping and relevant technical parameters.
- Assessment of potential cumulative effects from large-scale offshore wind development in Denmark and neighbouring countries.
- Assessment of barriers and potentials in relation to coexistence.

This report addresses one component of Task 3: Cumulative Impacts. Specifically, it provides an overview of areas within Danish offshore regions likely to be particularly affected by new offshore wind farm development, based on numerical simulations of wake losses from large offshore wind farms. All other tasks were finally reported in January 2026.

The overall project has primarily relied on historical data, with minimal new data collection. Consequently, the overall project sensitivity mapping largely depends on the availability and accessibility of existing data across specific subject areas. From the beginning, significant efforts were made to incorporate all relevant data to address the task requirements comprehensively. However, data from wind and other atmospheric parameters is used with minimal verification in the modelling tasks, mainly due to the lack of required data from existing wind farms. While power production data from Danish wind farms are available, other potential losses, such as curtailment and downtime for repairs, are not included, limiting their usefulness for verification. Wind measurements near existing wind farms are nearly always unavailable.

2 Introduction

In a previous report entitled "Environmental Mapping and Screening of the Offshore Wind Potential in Denmark Sensitivity mapping: Wind" [15], we reported on simulations of the atmospheric flow during 2019 to estimate the wind resources for the North Sea, the South Baltic Sea and the Kattegat using three scenarios: (i) no wind farms, (ii) wind farms as installed in November 2021, and (iii) future wind farm deployment in 2030. The simulation results are compared to understand the impact of wind farms on wind resources. All future wind farm scenarios were provided by the Danish Energy Agency (Energistyrelsen).

In a second report [13] entitled "Environmental Mapping and Screening of the Offshore Wind Potential in Denmark Sensitivity mapping: Comparison of Old and New Simulations", we updated the results using a set of revised simulations that included adjustments to the mesoscale model and UK offshore capacities. The main conclusion of this revised report is that, apart from the areas near the large UK offshore wind farms, where capacity densities were decreased, the conclusions of the first report remain valid.

In a third report [14] entitled "Interannual Variability of Wake Effects", we analysed the year-to-year variability in wind resources and wake impacts by examining five years of simulation results and comparing them to the single year previously simulated and presented in [13]. The analysis of these simulations showed that mean wind speeds in Danish waters vary annually by up to ±1 m s^{-1}, partly due to variations in the North Atlantic Oscillation, affecting energy output and wake losses in the Danish region. Yearly wind variability influences energy yield and load hours, with Danish yearly FLH ranging from 2990 (2021) to 3162 (2020). Simulated yields are higher than actual yields because they exclude real-world losses and mismatches in wind farm scenarios. Simulations with a wind farm scenario valid for November 2021 show that Danish wind farms cause a loss of power of 9–11 %, which doubles to 19–21 % under the 2030 scenario, with large regional variations. Percentage wake losses per year are generally higher with lower yearly mean wind speeds.

In this fourth and last report, we analyse two new sets of mesoscale model simulations using various hypothetical 2050 scenarios and two WRF model domain configurations with different grid spacings. In the first set, we compare the previously run scenarios for November 2021 and 2030 wind farms to the new 2050 scenario. Afterwards, we contrast the results of three new 2050 scenarios with the exact total installed capacity, but with different geographic distributions and capacity densities, on a new WRF model grid with increased spatial resolution. The purpose is not to assess the performance of individual wind farms, as the wind farm's layout in the North Sea has not yet been decided, but to draw conclusions regarding the advantages and disadvantages of various cluster layouts.

3 Mesoscale and wind farm model

The Weather Research and Forecasting (WRF) model [20] is an atmospheric mesoscale model that has become an essential tool for wind resource assessments [16], as evidenced by its use in the creation of modern wind atlases [3, 4, 6]. The WRF model can incorporate the effect of wind farms through a wind farm parameterisation (WFP). Several WFPs have been implemented, with the original implementation of the Fitch WFP [9] and the explicit wake parameterisation [EWP; 21] being the two most commonly used [8]. Both WFPs have been extensively discussed in the literature, and research findings are usually framed in comparisons of wind-speed-based wake extension, turbulent kinetic energy (TKE), and power production [1, 2, 11, 17, 19].

However, previous studies have shown that wind farm parameterisations exhibit various errors relative to observations across different regions of the wind farm, e.g., in internal versus external wakes. In [10], for a 6 x 6 turbine wind farm, the Fitch WFP produces wind speed deficits that are too deep in the first grid cell containing the wind turbine; however, agreement improves in downwind grid cells. By contrast, EWP yields much smaller wind-speed deficits in the grid cells containing the wind turbines, but the wake extends farther downstream. In a first attempt to verify against wind farm production data for the German Bight, Sengers and colleagues at the Fraunhofer Institute for Wind Energy Systems [18] showed that the EWP slightly overestimates production across all wind farms. In contrast, the Fitch WFP overestimates wind-speed deficits and underestimates energy yields. However, their conclusions cannot be extended to the very large wind farms simulated in the Y2030 and Y2050 scenarios, which have yet to be built. In this report, we present the Fitch modelling results first, followed by the EWP results. This order does not indicate which scheme is more accurate, but reflects the scheme most used in the scientific literature.

We conduct two new sets of mesoscale simulations for the 2050 scenarios using the same general WRF model configuration, but with different domain locations and grid spacings. In the first set, we use the previously employed domain (now referred to as the "Large domain" in this report and shown in Figure 1), covering the North Sea, the southern Baltic Sea, and the Kattegat with a 3 km x 3 km grid spacing and compare these results to those from previous scenarios documented in reports [13] and [14]. For this initial set, we employed both the Fitch [9] and EWP [21] wind farm parameterisations. This first set is intended to be compared with prior simulations for the CURRENT and Y2030 scenarios [13, 14]), and examines the influence of the Y2050 wind farm scenario on atmospheric flow, wakes, and Danish power output.

The second set utilises a newly defined domain called the "Small Danish domain" and is displayed in Figure 4, which covers a more limited area within the Danish North Sea, with a smaller spatial grid spacing of 1.5 km x 1.5 km. Once again, both the Fitch and EWP WFPs are used in this second set of simulations. The second set aims to identify the optimal installed capacity density and distribution of wind farms across the Danish North Sea, given the same installed capacity, primarily to reduce wake-induced power losses. An additional goal was to assess the impact of WRF model resolution on wake behaviour and recovery distances for similar wind farm configurations.

We describe these two WRF model configurations below.

3.1 The Large domain

The Large domain (Figure 1) was previously described in [13]. The Large domain 2050 simulations use the same WRF model configurations as in previous scenarios. We run the WRF model simulation on this domain, including an additional wind farm deployment scenario for 2050 (Table 2). We compare simulations under the 2050 (Y2050) scenario with those under the NoWF, CURRENT, and Y2030 scenarios. In the simulations that include wind farms, we introduce the effect of the wind turbines with the distribution of wind turbines as shown in Figure 2. The land-based wind turbines do not change between the CURRENT, Y2030 and Y2050 scenarios. The total installed capacities in these scenarios are summarised in Table 2. For verification purposes, it is worth noting that the CURRENT scenario for 2021 is the most accurate reflection of the system's actual state, as the meteorological conditions align with those of the wind farm.

The geographical distribution of the installed capacity for each scenario is shown in Figure 2. For

Table 1: Scenarios used in the WRF model simulations with the Large domain. The EWP simulations use the EWP wind farm parameterisation to provide a comparison and alternative context for viewing the model results from wind farm parameterisations.

Simulation	Wind farm scenario	Meteorological year
NoWF	No wind farms	2019
CURRENT	Wind farms as of Nov 2021	2019
Y2030	Wind farm scenario 2030	2019
Y2050	Wind farm scenario 2050	2019
EWP_CURRENT	As CURRENT, but using EWP	2019
EWP_Y2030	As Y2030, but using EWP	2019
EWP_Y2050	As Y2050, but using EWP	2019

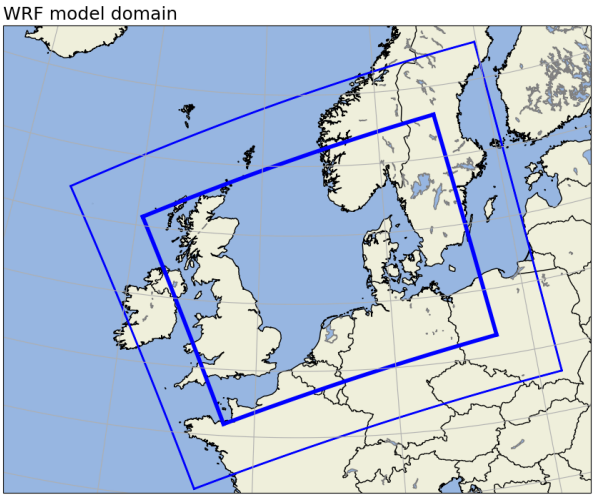


Figure 1: Geographic location of the Large domain used in the simulations. The thick blue line outlines the region where the wind farms are added, and the results are analysed.

Table 2: Installed capacity (in GW) per country in the CURRENT (November 2021), Y2030, and Y2050 scenarios in the WRF model domain. A fixed onshore installed capacity is used in all scenarios.

Country	Onshore (All) [GW]	Offshore CURRENT (2021) [GW]	Offshore Y2030 [GW]	Offshore Y2050 [GW]
DK	4.2	2.3	17.0	47.4
SE	3.6	0.1	2.4	2.4
DE	36.4	7.3	29.4	70.0
UK	9.0	10.2	59.5	93.7
NL	2.7	2.6	38.1	40.2
NO	1.2	–	10.0	19.0
PL	1.0	–	–	–
BE	1.4	2.3	2.3	5.1
FR	1.6	–	–	8.5
Total	61.2	24.8	158.7	286.3

2050, Figure 2 shows that most new wind farms are located in the south and west North Sea, further offshore than in the Y2030 scenario. There are also new additions in the UK (34 GW), mostly east of Scotland. In this scenario, Denmark adds 30.4 GW, while Germany adds 40.6 GW of new offshore wind capacity. The largest cluster of wind farms is now located north of the German Bight. Norway adds one large offshore wind farm of 9 GW capacity offshore along the border with Denmark.

All future wind farms for the 2030 scenario use the IEA 15 MW wind turbine characteristics (Figure 3a) with hub height of 145 m and rotor diameter of 235 m; all future wind farms for the 2050 scenario use a hypothetical 27 MW wind turbine (Figure 3b) with hub height of 180 m and rotor diameter of 300 m. The 27 MW power and thrust curves were created with PyWake using their generic CT/CP generator [23].

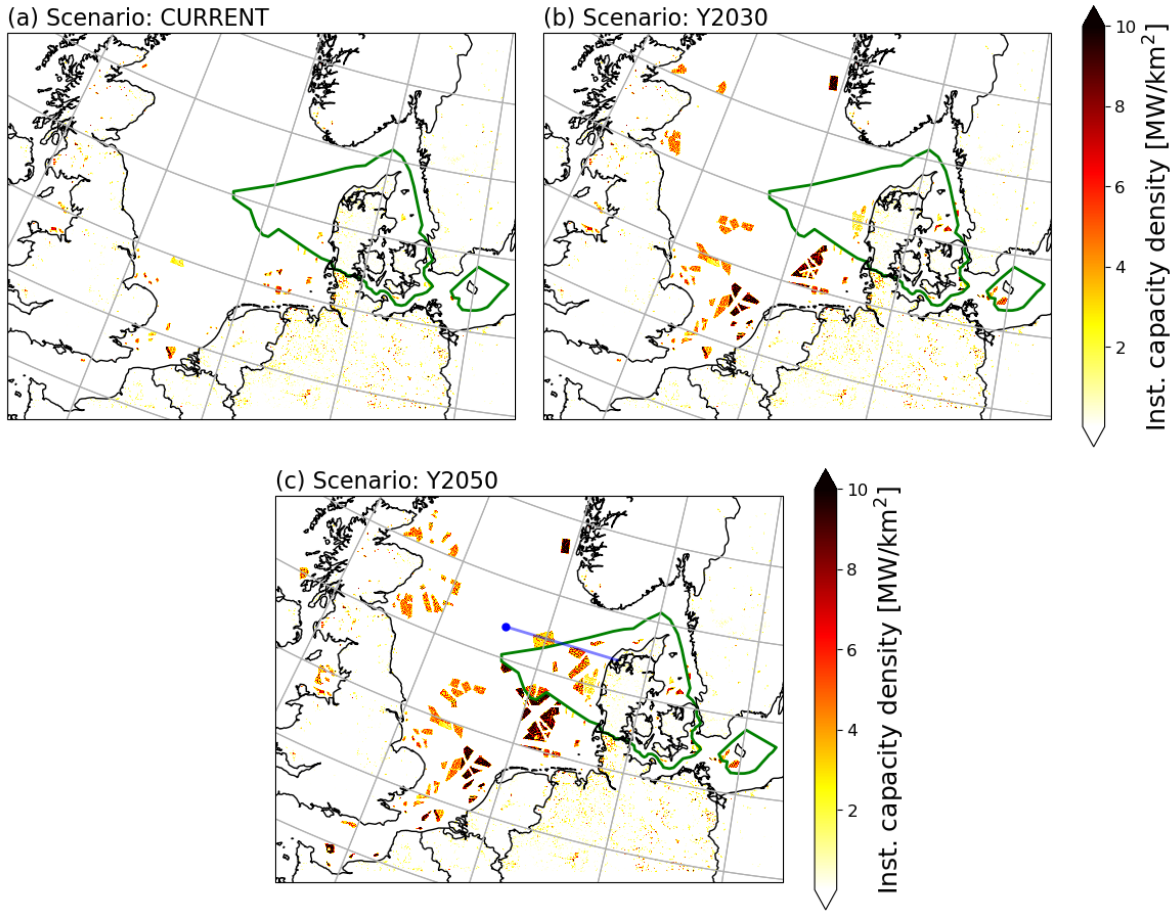


Figure 2: Installed capacity density [MW km^{-2}] in each WRF model grid cell (3 km × 3 km) in the simulations: (a) CURRENT, (b) Y2030 and (c) Y2050 wind farm scenarios. The green line shows the Danish EEZ. The blue line shows the transect location, which starts at the blue dot and is analysed in Sec. 4.3.

3.2 The Small Danish domain

In the Small Danish domain, we used a WRF model domain nearly identical to the one used in the Large domain, centred in the North Sea (Figure 4) and rotated it to maximise coverage of the Danish North Sea, including some major future wind farms in Germany and Norway. The domain rotation is identical to that of the Large Domain. We used two nested inner domains to increase the model grid spacing incrementally from the 27 km of the ERA5 reanalysis. The grid spacing of the domains is 13.5 km by 13.5 km (d01), 4.5 km km by 4.5 km (d02), and 1.5 km by 1.5 km (d03) in the innermost domain. In this inner domain, the wind farms are introduced, and the results are analysed. The area of interest was selected based on Figure 7 and Figure 21 to include all areas where, from the Large domain simulations, the capacity factors return to 98 % of the NoWF scenario.

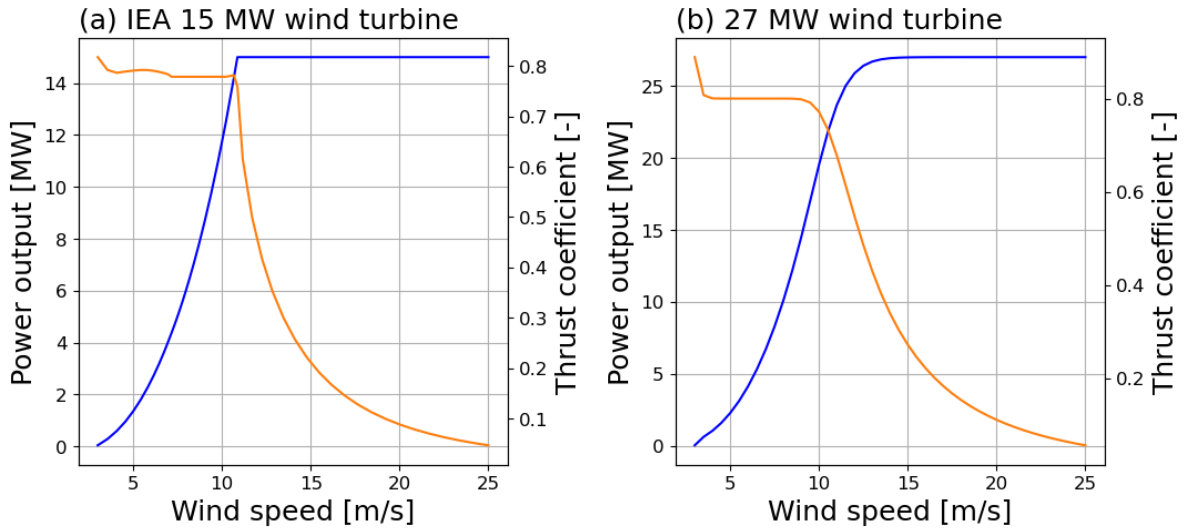


Figure 3: Power (in blue) and thrust (in orange) curves for the (a) IEA 15 MW and (b) hypothetical 27 MW [23] wind turbines.

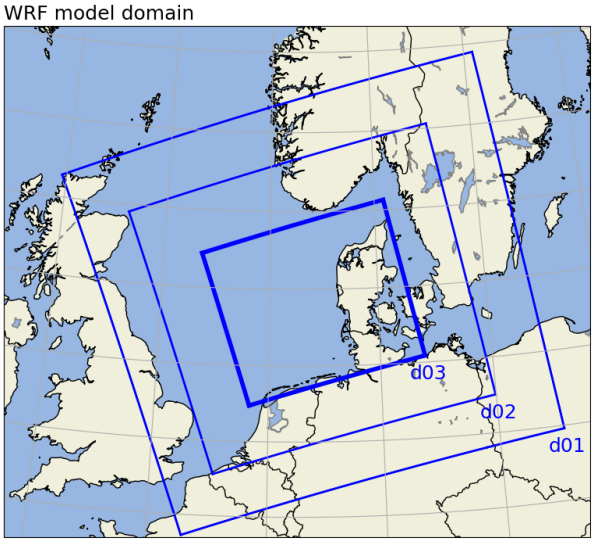


Figure 4: Geographic location of the Small Danish domain used in the simulations. The thick blue line outlines the region where the wind farms are added (d03), and the results are analysed.

Table 3: Wind farm scenarios used in the WRF model simulations with the Small Danish domain. Simulations were run with both the Fitch and EWP wind farm parameterisations.

Simulation	Wind farm scenario	Meteorological year
CURRENT	Wind farms as of Nov 2021	2022
Y2050_SCE1	Scenario 1 – low installed capacity	2022
Y2050_SCE2	Scenario 2 – small dense WFs	2022
Y2050_SCE3	Scenario 3 – German WFs	2022

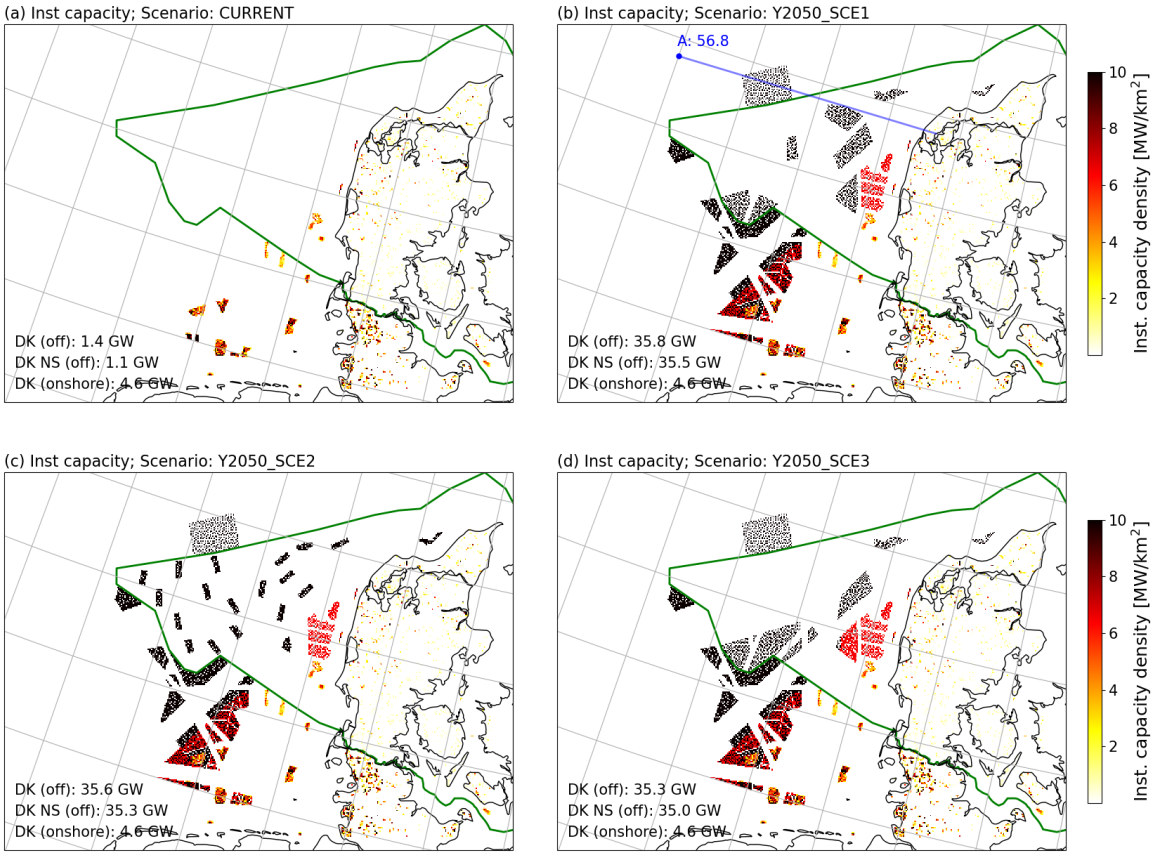


Figure 5: Installed capacity density [MW km^{-2}] in each WRF model grid cell (1.5 km $\times$ 1.5 km) in the CURRENT and three future Y2050 scenarios (Table 3). The green line shows the Danish EEZ. The values in the bottom-left corner are the total installed capacity in Denmark for each scenario, while the blue line in (b) shows the transect location, which starts at the blue dot and is analysed in Sec. 4.3.

The three 2050 scenarios (Table 3) were designed to determine which WF distribution is most efficient for energy production and wake minimisation. The installed capacities for these scenarios are shown in Figure 5. All scenarios have a total installed capacity near 35 GW (35.5 GW in SCE1, 35.2 GW in SCE2, and 35.0 GW in SCE3). The Y2050_SCE1 simulation shows large WFs with low capacity density (5.2 MW km^{-2}), mainly in the low-lying areas of the Danish EEZ. This configuration reduces foundation costs [7]. The Y2050_SCE2 simulation has smaller WFs with high power density (10 MW km^{-2}) scattered through the North Sea Danish EEZ. Many of these 16 small WFs are located in the northern part of the EEZ. The Y2050_SCE3 simulation includes WFs with low power density (5.2 MW km^{-2}) located close to the Danish and German coasts, thereby reducing cabling costs. The Y2050_SCE1 scenario is closest to the Y2050 scenario used in the Large domain simulations. As in the Large Domain, all future wind farms for the 2050 scenario use a 27 MW wind turbine characteristics (Figure 3b).

We run these simulations for 2022 rather than 2019, as previously done, for two reasons. First, lidar measurements of the coast of Jutland, commissioned by Energinet.dk [15], can be used to validate the undisturbed flow in these simulations. These measurements started in December 2021. Secondly, 2022 is more in line with the CURRENT wind farm scenario for November 2021, facilitating a general comparison with power data, which will be done later for an academic publication of the results.

4 Results

As in the previous section for the model setup, we present the results separately for the Large and Small Danish domains.

4.1 The Large domain

As in previous reports, we present the analysis of results for a smaller Danish-centred focus area than the whole inner domain. Figures for the whole domain are available in Annex 1.

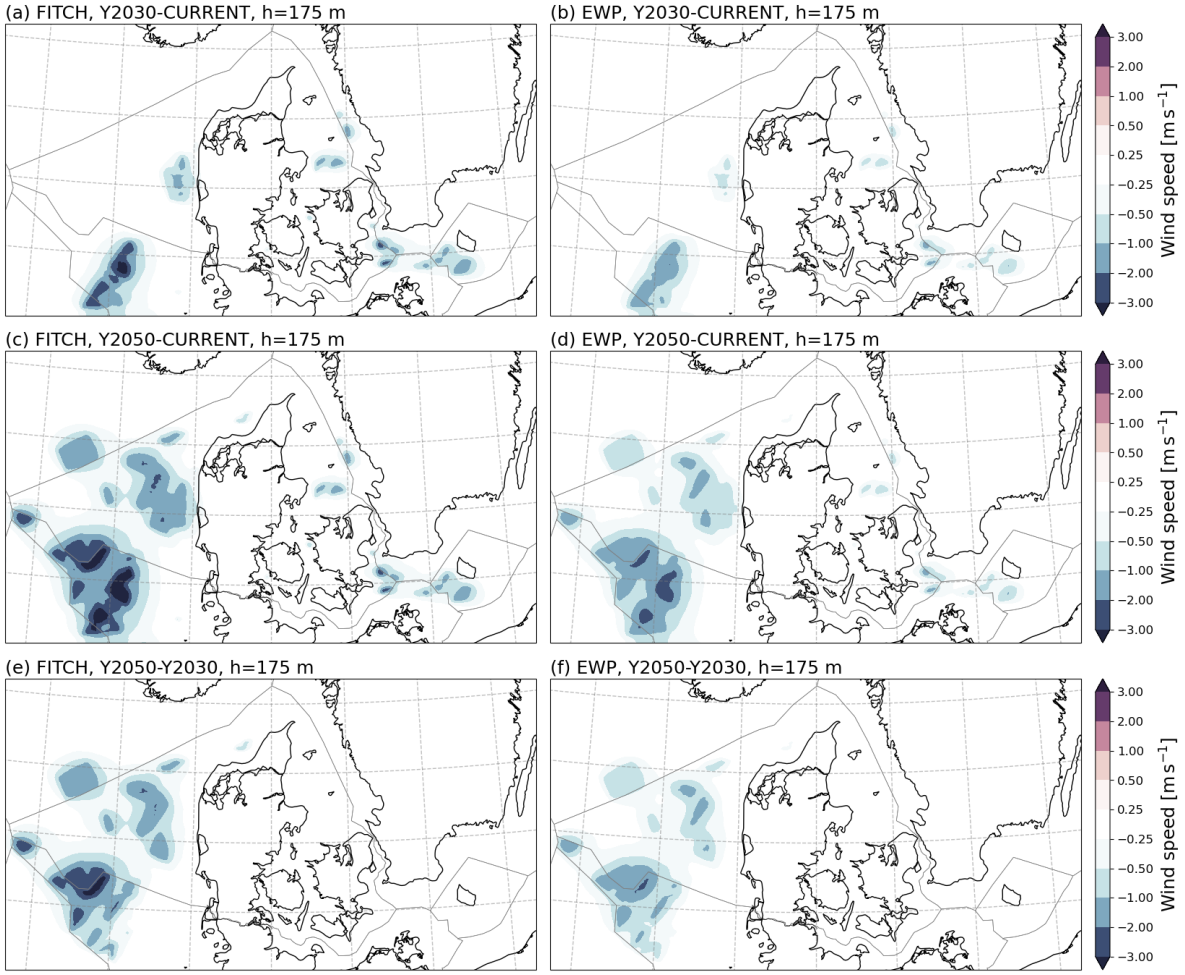


Figure 6: Difference in mean wind speed [m s^{-1}] at 175 m AGL for all 2019 between various wind farm scenarios and WFPs: (a,b) Y2030 minus CURRENT for FITCH and EWP, (c,d) Y2050 minus CURRENT for FITCH and EWP, and (e-f) Y2050 minus Y2030 for FITCH and EWP.

Figure 6 shows the wind speed differences at 175 m AGL, the level closest to the hub height of the wind turbines used in the Y2050 scenario, between the various simulations for the Fitch and EWP wind farm parameterisations. In the Y2050 scenario for the Fitch WFP, decreases in wind speed are of the order of −3 m s^{-1} in the southwestern border of the EEZ, but only exceed −2 m s^{-1} in the centre of the new Danish wind cluster. Decreases are of small magnitude for the simulations using the EWP WFP.

By comparing Figure 6a and Figure 6c, and by examining the differences between the Y2030 and Y2050 scenarios in Figure 6e, it is possible to see how the wind speed deficits superimpose as new wind farms are built, thereby enhancing their effects. In the Y2030 scenario, the wind speed contour of −0.25 m s^{-1} is confined to a small area offshore in the North Sea. In the Y2050 scenario, deficits combine, and nearly half of the Danish EEZ experiences a decrease (<−0.25 m s^{-1}) in mean wind

speed, extending westward from the new Norwegian wind farm. In the south, the new German wind farms also contribute to reduced mean wind speeds in the Danish EEZ. This is better seen in Figure 7, which shows the capacity factors.

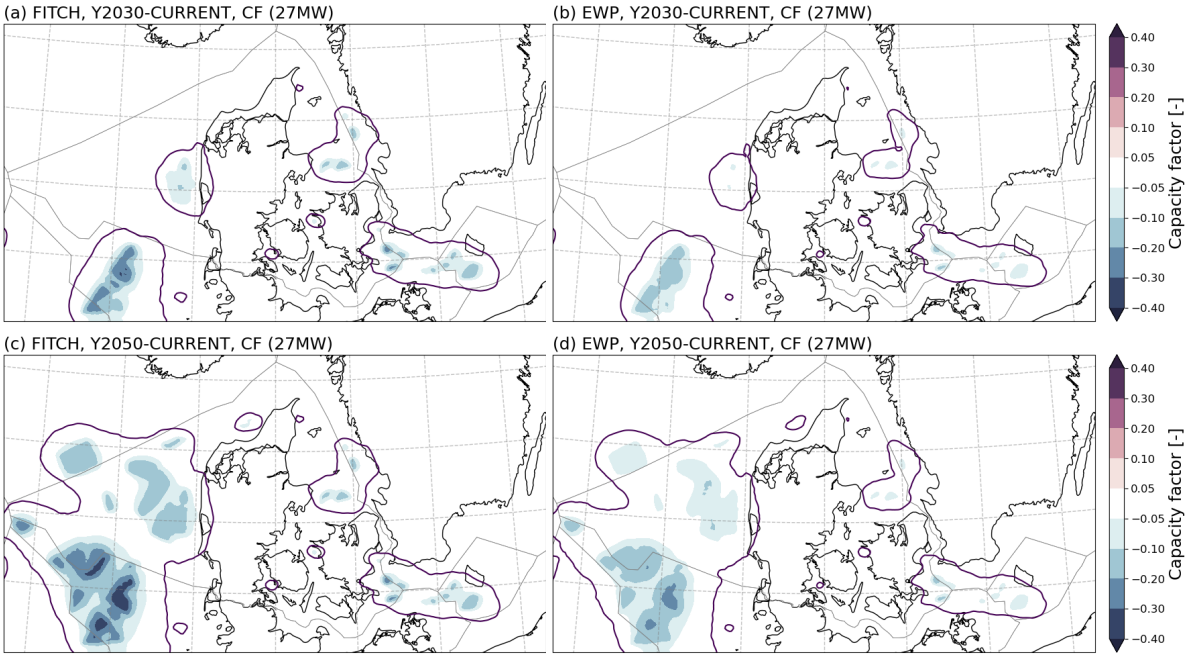


Figure 7: Difference in mean capacity factor [-] from the CURRENT wind farm scenario for all 2019 for the hypothetical 27 MW wind turbine for the following scenarios and WFPs: (a) Y2030, Fitch, (b) Y2030, EWP, (c) Y2050, Fitch, (d) Y2050, EWP. The purple line on each figure shows the wake recovery at 98 % from the CURRENT scenario.

Figure 7 shows the difference in capacity factor for the new hypothetical wind turbine used in the Y2050 scenario. The influence of the extensive new wind farms in the Y2050 scenario is reflected in the differences in mean wind speed. Differences in CF are as large as −0.25 in the southern Danish North Sea EEZ. The 98 % wake recovery line covers most of the Danish EEZ, but does not extend further inland than in the Y2030 scenario. The differences in 27 MW capacity factors for the EWP parameterisation are smaller than those for the simulations using the Fitch parameterisation, but the line of wake recovery at 98 % is remarkably similar.

Surface climate changes

The simulations show very small changes in surface climate, similar to but more extensive than those found in the Y2030 scenario [14]. Figure 8 shows differences in air temperature measured at 2 m AGL (2-m temperature for short) for the simulations using the Y2030 and Y2050 wind farm scenarios. In the Y2030 scenario, there is cooling offshore (−0.07 ˚C) in all seasons. During the summer, both scenarios show slight land warming, with the Y2050 scenario also showing warming in northern Jutland. These changes are unlikely to be statistically significant at the 95 % confidence level (which should be tested in the future).

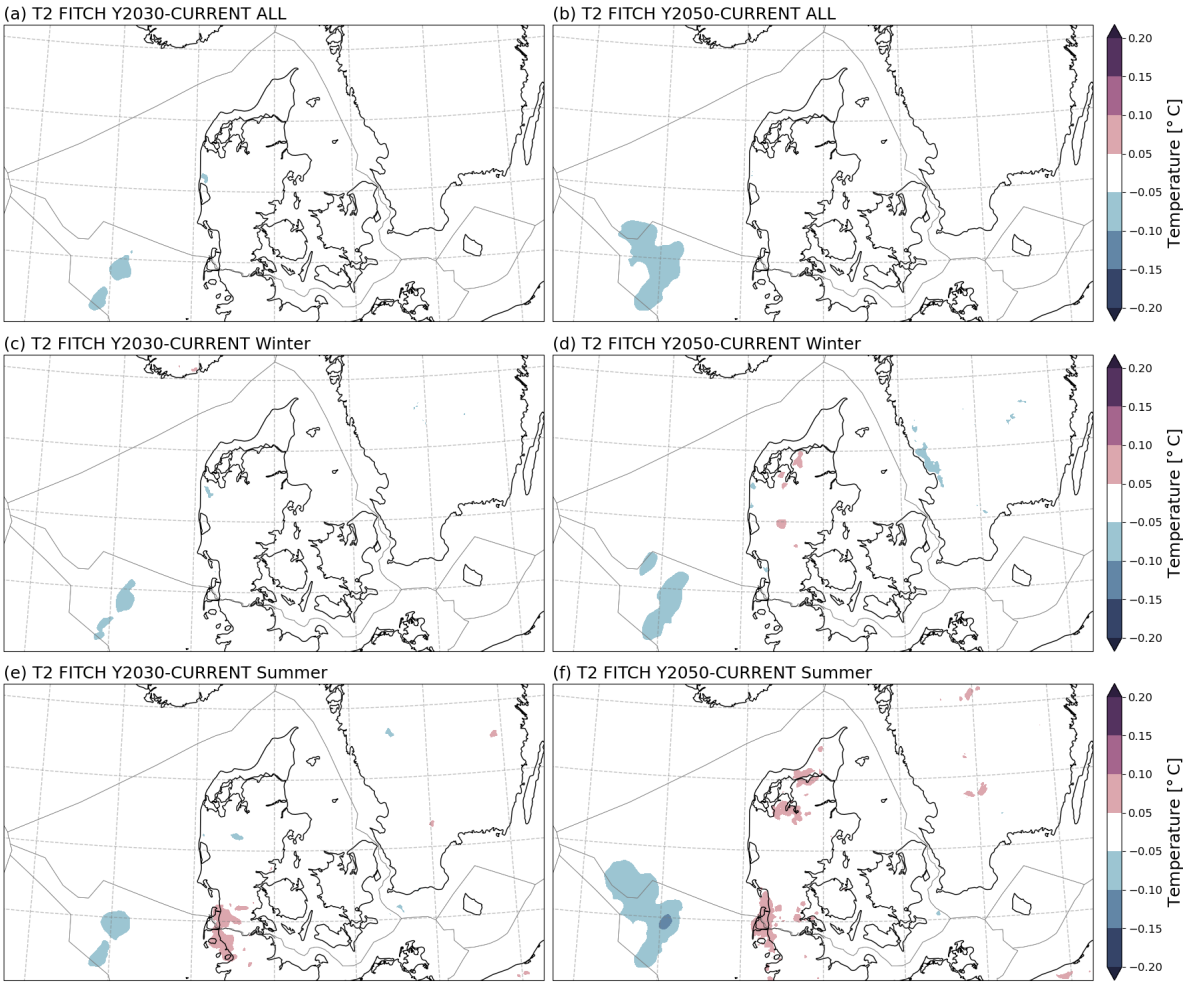


Figure 8: Difference in mean 2-meter temperature [˚C] from the CURRENT simulation for the Y2030 (left) and Y2050 (right) for 2019 for the Fitch WFP for the full year (a and b), winter (c and d) and summer (e and f).

The simulations using the Y2030 and Y2050 scenarios show increases in boundary layer height above all large offshore clusters in the North and Baltic Seas (Figure 9). The increases, between 40 m to 80 m, are larger in summer than in winter; the increases also cover a larger area in summer and appear to be independent of the installed capacity density of the wind farms. These changes are statistically significant at the 95 % level, and no changes in boundary layer height are simulated over land.

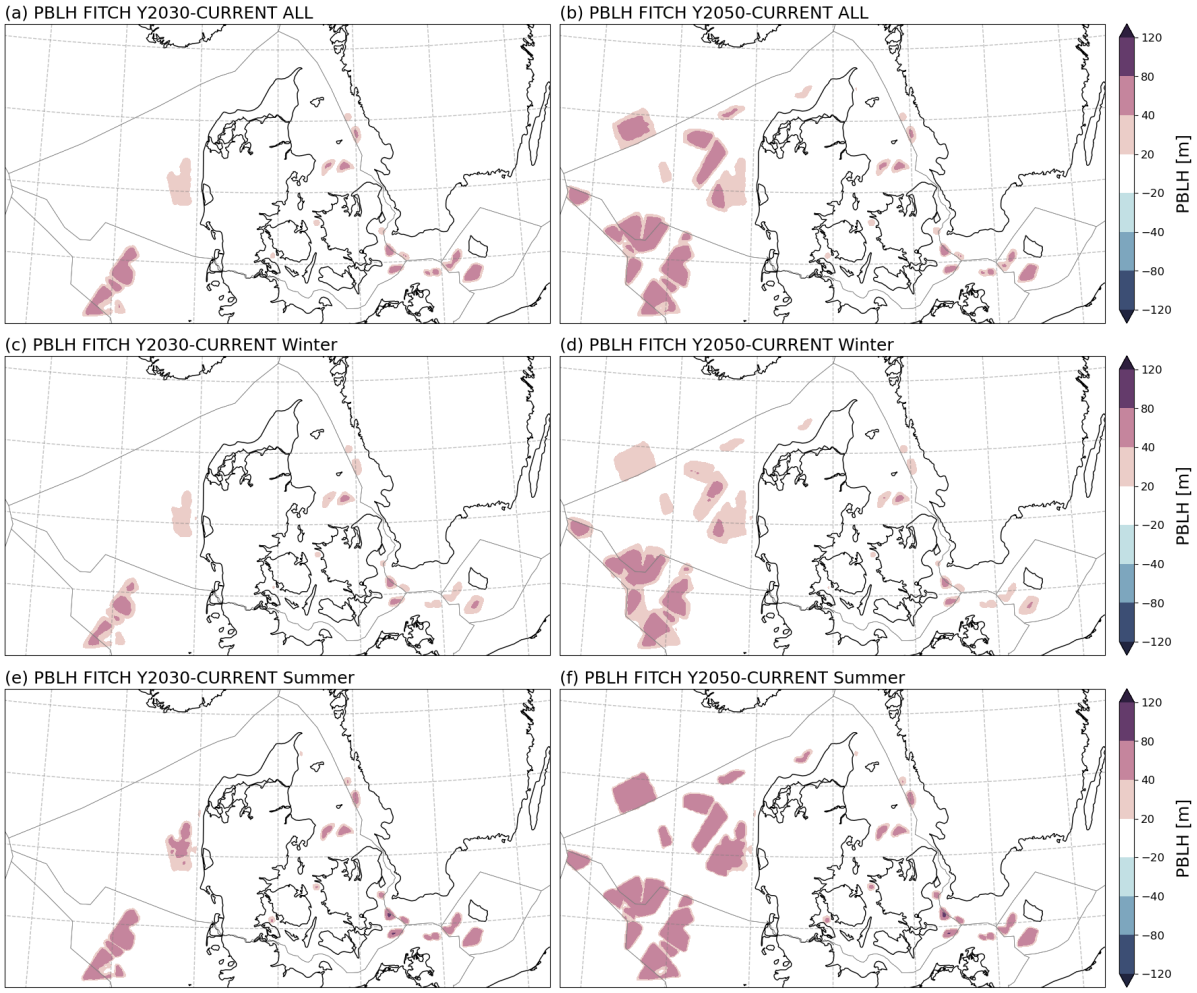


Figure 9: Difference in mean boundary layer height [m] from the CURRENT simulation for the Y2030 (left) and Y2050 (right) for 2019 for the Fitch WFP for the full year (a and b), winter (c and d) and summer (e and f).

The WRF model also estimates the fraction of the grid box covered by clouds. This value is determined by a random overlap of the cloud fraction at each model layer (variable CLDFRAC2D in the WRF model output). The changes in this quantity are shown in Fig. 10. The simulations show increases in cloud fraction, principally in the Y2050 scenario, near large wind farms, especially in summer. In both summer and winter, the largest increases are around 4 %. There are also extensive decreases in cloud fraction in areas downstream of the wind farms. Further analysis shows that these changes occur mainly in the lower clouds, typically below 300 m AGL, as one would expect, since turbines should modify the lower clouds only [5]. Unlike temperature changes, some of these areas may show statistically significant changes, but this needs to be tested.

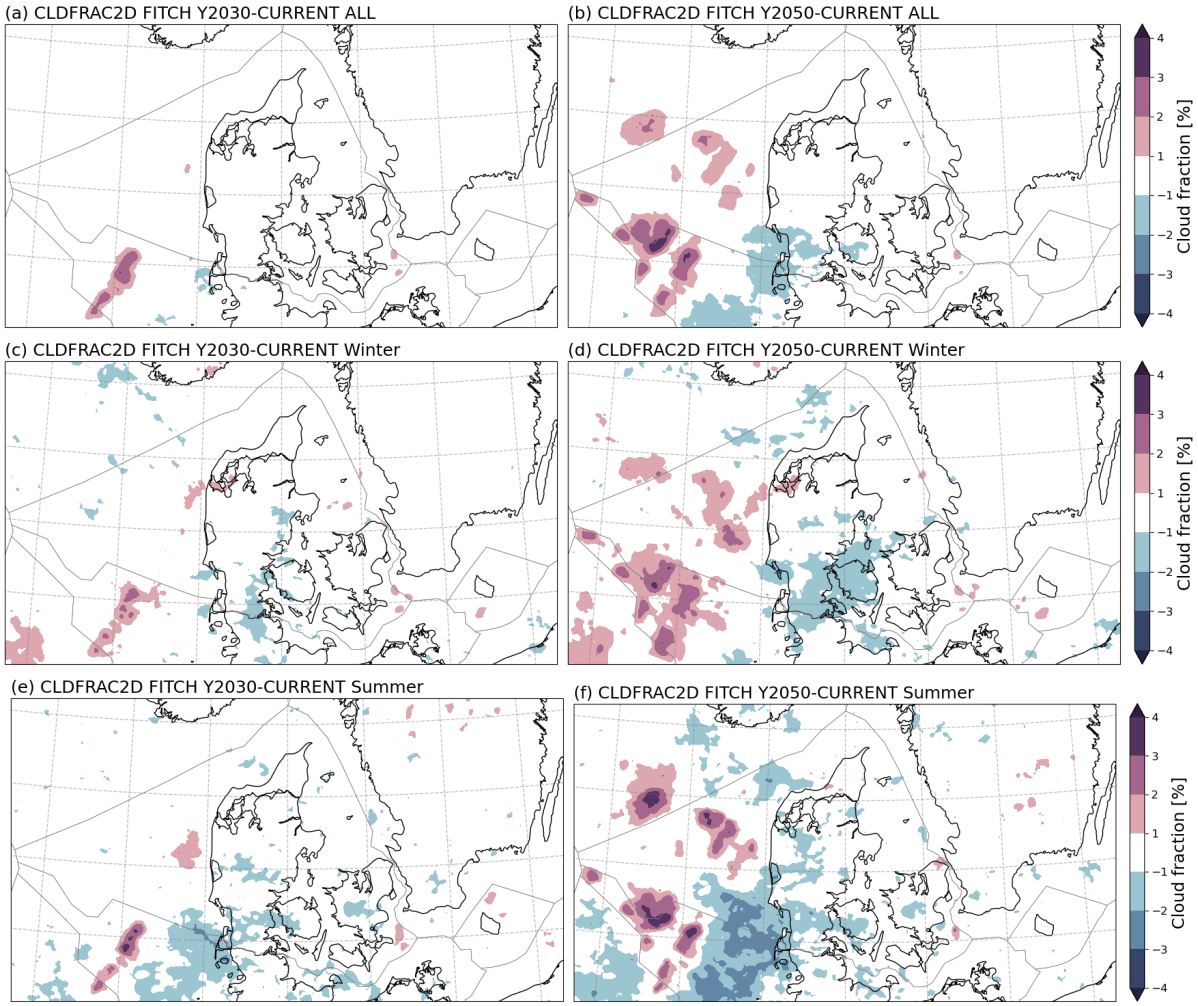


Figure 10: Difference in mean total cloud fraction [%] from the CURRENT simulation for the Y2030 (left) and Y2050 (right) for 2019 for the Fitch WFP for the full year (a and b), winter (c and d) and summer (e and f).

Power yield and wake losses

To evaluate how WRF-simulated wakes may influence power output, we provide estimates of full-load hours (FLH) per turbine based on the wind speeds simulated for each scenario in Table 1. Full-load hours are determined by dividing the estimated annual energy production, obtained from the wind turbine power curve, by the turbine's nominal power. The maximum possible FLH is 8766, corresponding to a turbine operating at full power for every hour of the year. We also include capacity factors (CF), with a 50 % CF equating to 4383 FLH. Additionally, we present wake losses, calculated as the relative difference in full-load hours between each scenario and the control (CURRENT) scenario without wind farms, sometimes referred to as wind farm efficiency [22].

The rated power of the wind turbines used in the simulations and scenarios is shown in Figure 11. This can serve as a proxy for the scenarios. The yellow markers represent the turbines in the Y2030 scenario (15 MW), and the dark red markers represent those in the Y2050 scenario (27 MW). Other green and blue points represent land-based turbines and offshore wind farms in the CURRENT scenario.

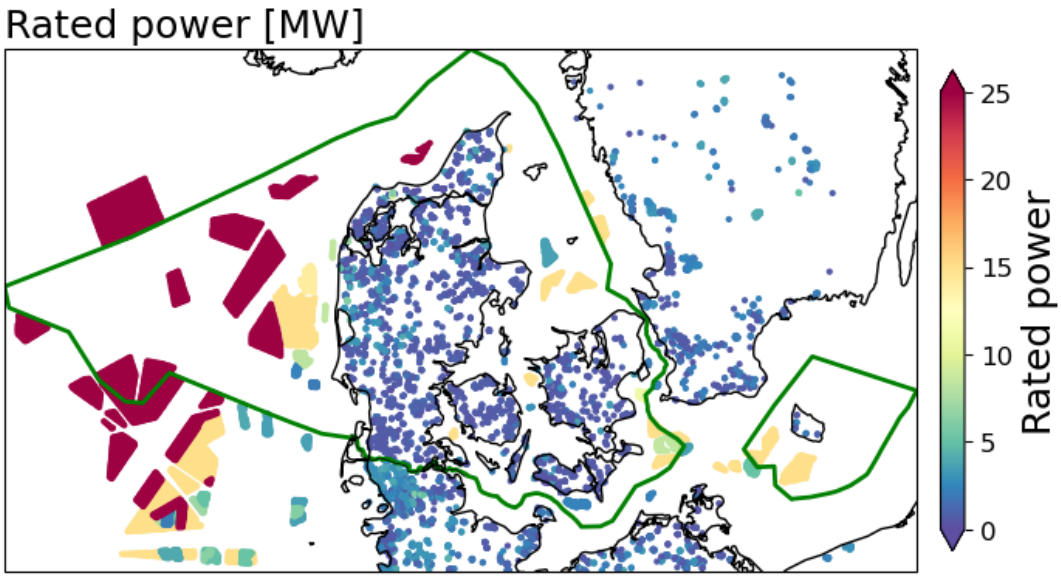


Figure 11: Rated power [MW] for all turbines used in the different scenarios. Yellow markers are for the Y2030 scenario (15 MW) and dark red for the Y2050 scenario (27 MW). Other colours represent turbines on land and the CURRENT scenario.

The FLH are calculated by estimating the power a given turbine will generate when subjected to the wind speed simulated at the height of the wind turbine rotor, rather than from the power output derived from the WRF model simulations, which can only be computed when the wind turbines are included in the simulation. Regardless of the source, these values include the large-scale wake when the WFP is utilised but exclude other losses such as turbine availability, electrical efficiency, performance, environmental factors, or curtailments. Additionally, some turbine-to-turbine interactions are not accurately simulated by the WFPs when the wind turbines are located within the same WRF model grid cell; this is common at 3 km x 3 km grid spacing. Both WFPs assume that all wind turbines are located at the centre of the grid cell and that there are no wake effects within the grid cell. This assumption can lead to inaccuracies, as turbines are often not perfectly aligned to avoid wake effects, resulting in overestimates of wind turbine impacts (e.g., power).

The FLH for the Y2030 and Y2050 scenarios are presented in Figure 12, comparing the results from the two wind farm parameterisations. In the simulations that do not account for wakes, nearly all large wind farm clusters in the North Sea away from the coast have more than 5000 FLH. These values appear rather large because they exclude all losses; the winds at 175 m are strong and steady, resulting in a CF close to 0.6. Any variation in FLH before accounting for wakes is due to the variation in wind resource (due to spatial variation in wind climate) or due to a different turbine power curve. The FLHs are markedly reduced in both scenarios, but mainly in the Y2050 scenario. The wind turbines in Danish wind farms close to the German border drop their electricity production by 25 to 30 % in the Fitch and 15 to 20 % in the simulation using EWP parameterisations, respectively. Some wind farms present in the Y2030 scenario suffer from the build-up of new wind farms in the Y2050 scenario.

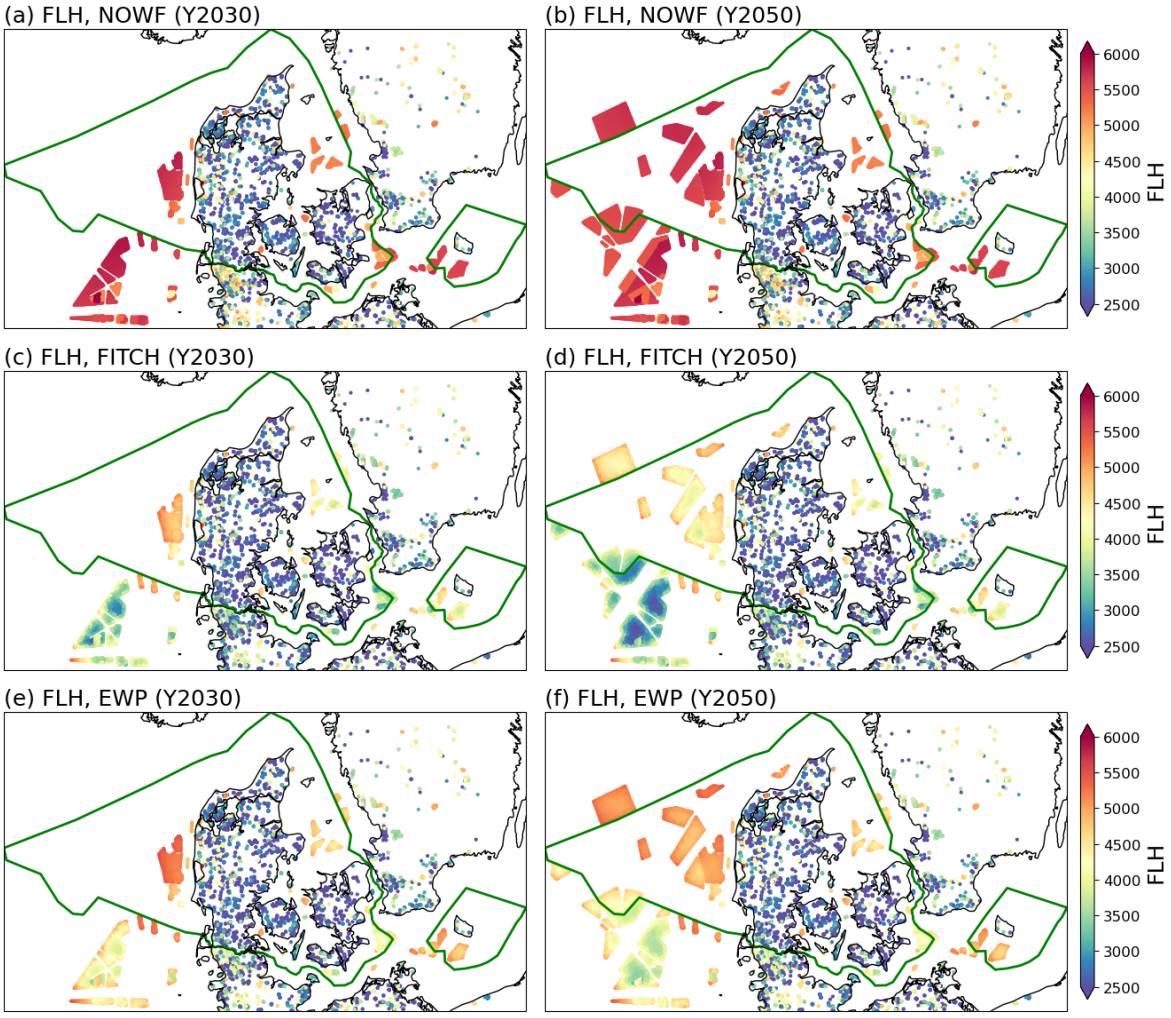


Figure 12: Annual FLHs [h] per wind turbine in the Y2030 (left) and Y2050 (right) wind farm scenarios for 2019 using (a,b) No wind farm (NoWF), (c,d) FITCH, and (e,f) EWP WFPs.

Figure 13 shows the wake losses from the scenario without wind farms and in the various future scenarios of the WRF model simulations. In the Y2050 scenario in the Danish EEZ, wake losses are between 10 % to 30 %, except for the Baltic Seas, where Danish and German wind farms lie very close to each other. There are also wake losses over land near the west coast of Jutland, but they remain relatively constant between the Y2030 and Y2050 scenarios. However, this highlights the need to carefully consider the layout of future wind farms close to the coast.

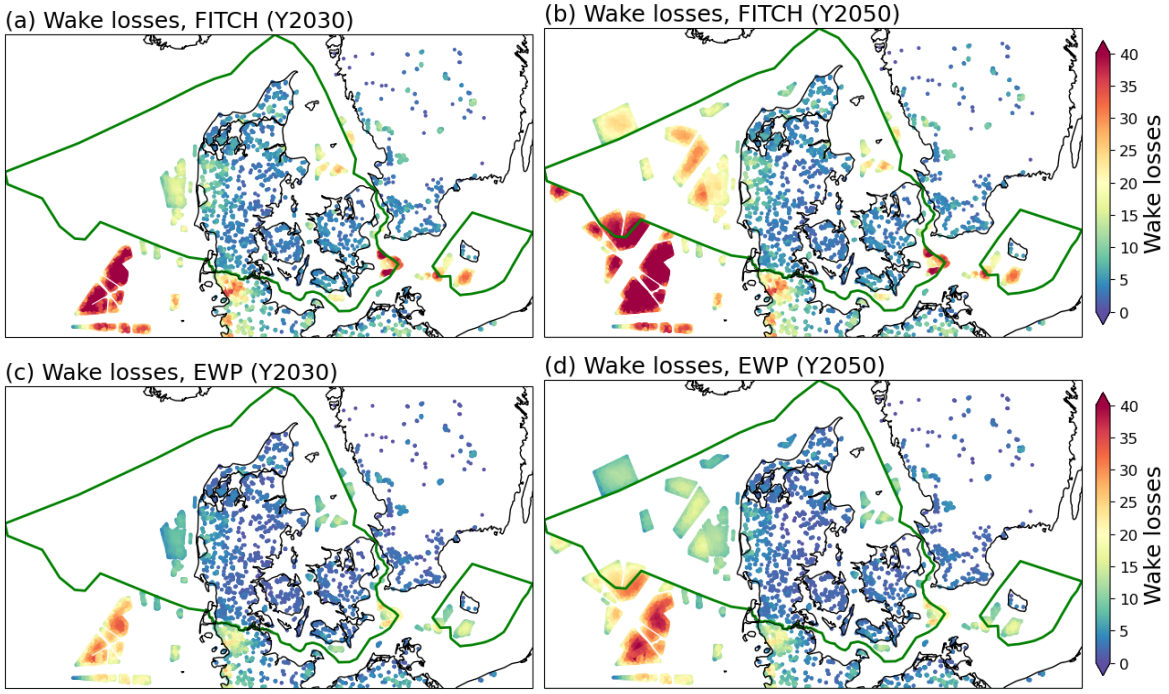


Figure 13: Wake losses [%] per wind turbine in the Y2030 (left) and Y2050 (right) wind farm scenarios for 2019 using the (a,b) FITCH, and (c,d) EWP WFPs.

The annual power values estimated from the CURRENT, Y2030, and Y2050 simulations are shown in Table 4. Average full load hours in the simulations without wake effects range from 3258 in the CURRENT scenario to 4034 in the Y2050 scenario. These values result from increased installed capacity in the future scenarios. Annual energy yields are estimated as 23.1 TW h to 24.4 TW h in the CURRENT scenario using the Fitch and EWP WFPs, respectively. Yields increase in the future scenarios, from 84.5–94.4TW h in the Y2030 to 203.8–232.5TW h in the Y2050 scenarios, despite overall larger wake losses.

Wake losses are computed by comparing the AEP with and without wakes. The wake losses are estimated as 13.7 % in the Y2050 scenario using the EWP WFP, only 2.3 % higher than in the Y2030 scenario. This is due to a low installed capacity density in the Y2050 scenario and the placement of future wind farms in areas with excellent wind resources, farther from the coast. This means that by building either smaller wind farms or low-density wind farms, Denmark can scale up wind farm deployment in the North Sea without compromising overall yield. These results are highly dependent on the wind farm configuration in the future scenarios, as will be shown in the next section, which focuses on the Small Danish domain.

Table 4: Annual mean full load hours, total power yield [TW h], mean capacity factor [%], and mean wake losses [%] of all Danish turbines across the various simulated scenarios for 2019. These values do not account for additional losses due to turbine availability, electrical efficiency, performance, environmental factors, or curtailments.

Wind farm scenario	WFP	FLH	AEP [TW h]	CF [%]	Wake loss [%]
CURRENT	NoWF	3258	25.8	37.2	–
CURRENT	Fitch	3009	23.1	34.4	10.4
CURRENT	EWP	3124	24.4	35.7	5.5
Y2030	NoWF	3697	106.4	42.2	–
Y2030	Fitch	3218	84.5	36.7	20.7
Y2030	EWP	3430	94.4	39.2	11.4
Y2050	NoWF	4049	277.8	46.2	–
Y2050	Fitch	3370	209.8	38.5	24.5
Y2050	EWP	3664	239.6	41.8	13.7

4.2 The Small Danish domain

In this section, we present the results of the Small Danish domain simulations for runs using both the FITCH and EWP WFPs. We focus on wind speed and power-related quantities. Variations in climate variables are similar across the Large and Small Danish domain simulations.

Mean wind speed and capacity factors

Figure 14 shows the difference in annual mean wind speed at 175 m AGL between the three 2050 scenarios and the simulation using the CURRENT wind farm scenario. Wind speeds decrease by as much as −3.7 m s^{-1} (or −35 %) in the regions with high capacity densities south of the EEZ German border. In the Danish EEZ, differences in mean wind speed are mostly no larger than −1.0 m s^{-1} (∼10 %), except for the core of the wind farms, where wind speed differences can reach −3.0 m s^{-1} (∼30 %) in the simulations using the Fitch WFP. The scenario Y2050_SCE2 has the largest area affected by decreases of at least −0.5 m s^{-1}, but fewer areas with very large decreases in wind speed. In the simulations using the EWP scheme, decreases in wind speed are smaller than in the Fitch scheme, with maximum decreases no greater than −1.0 m s^{-1} to −2.0 m s^{-1} in SCE1 and SCE3.

Figure 15 shows the differences in capacity factor due to the presence of wind farms in the 2050 scenarios. Most areas in the Danish EEZ limit the decrease in CF to less than −0.1, except for the wind farm areas, where it can reach between −0.2 and −0.3. This figure also shows the area affected by wind farms as identified by the 98 % recovery to the CF of the CURRENT scenario. As in the Large domain simulations (Figure 15), in the Y2050_SCE2 scenario, most of the Danish North Sea is affected by wind farms. The effect on land is nearly identical in the three scenarios. The Norwegian wind farm along the northern EEZ border does not significantly influence the Danish offshore wind farms except for a few small wind farms in the Y2050_SCE2 scenario. In the EWP simulations, the decreases in CF are reduced by a factor of 2, similar to the results in the Large domain. As previously highlighted in [13], the 98 % lines are nearly identical in the analogous simulations with the EWP parameterisation.

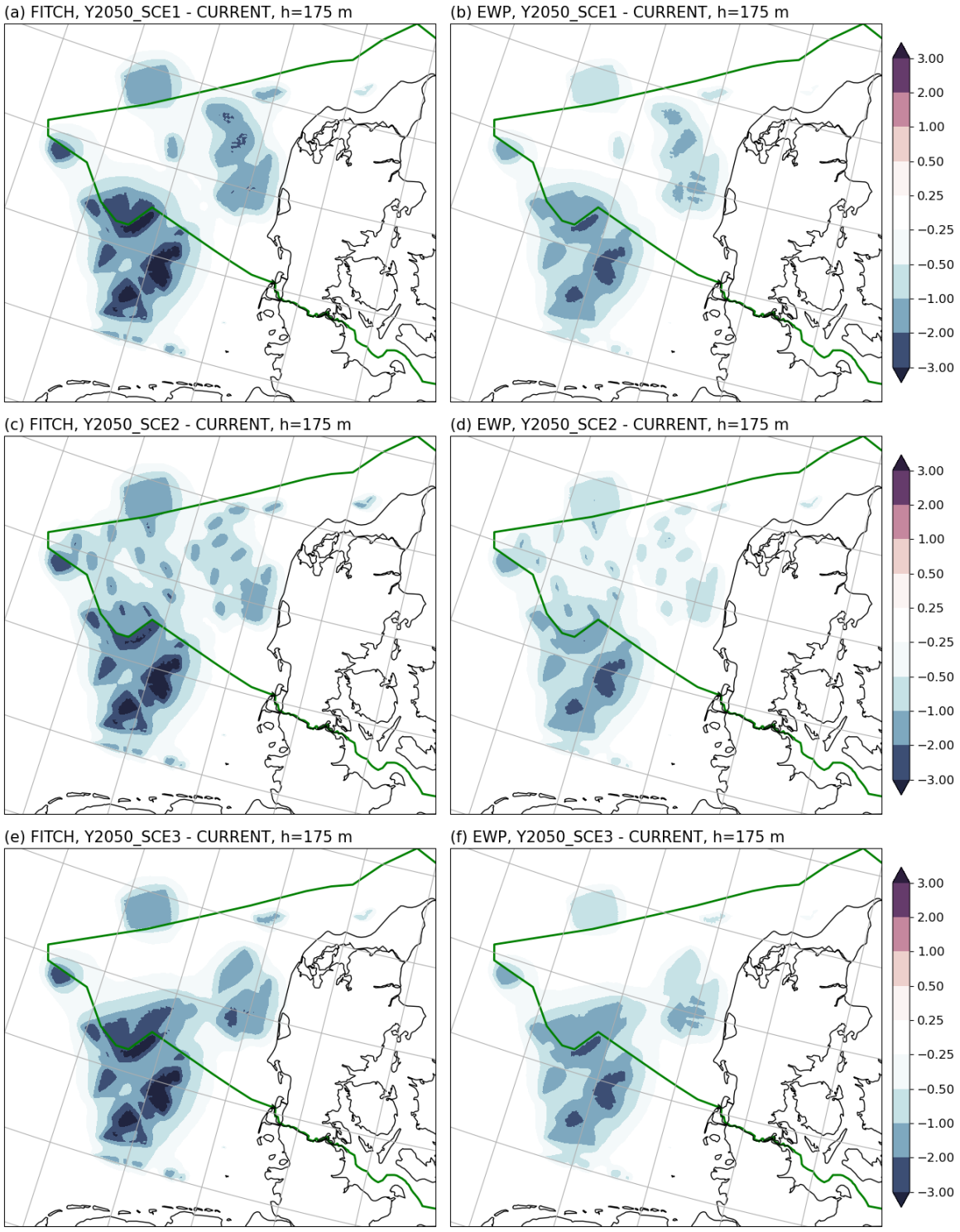


Figure 14: Difference in annual mean wind speed [m s^{-1}] at 175 m AGL from the CURRENT wind farm scenario for all 2022 for the three Y2050 scenarios for the FITCH (a, c, e) and EWP (b, d, f) WFPs.

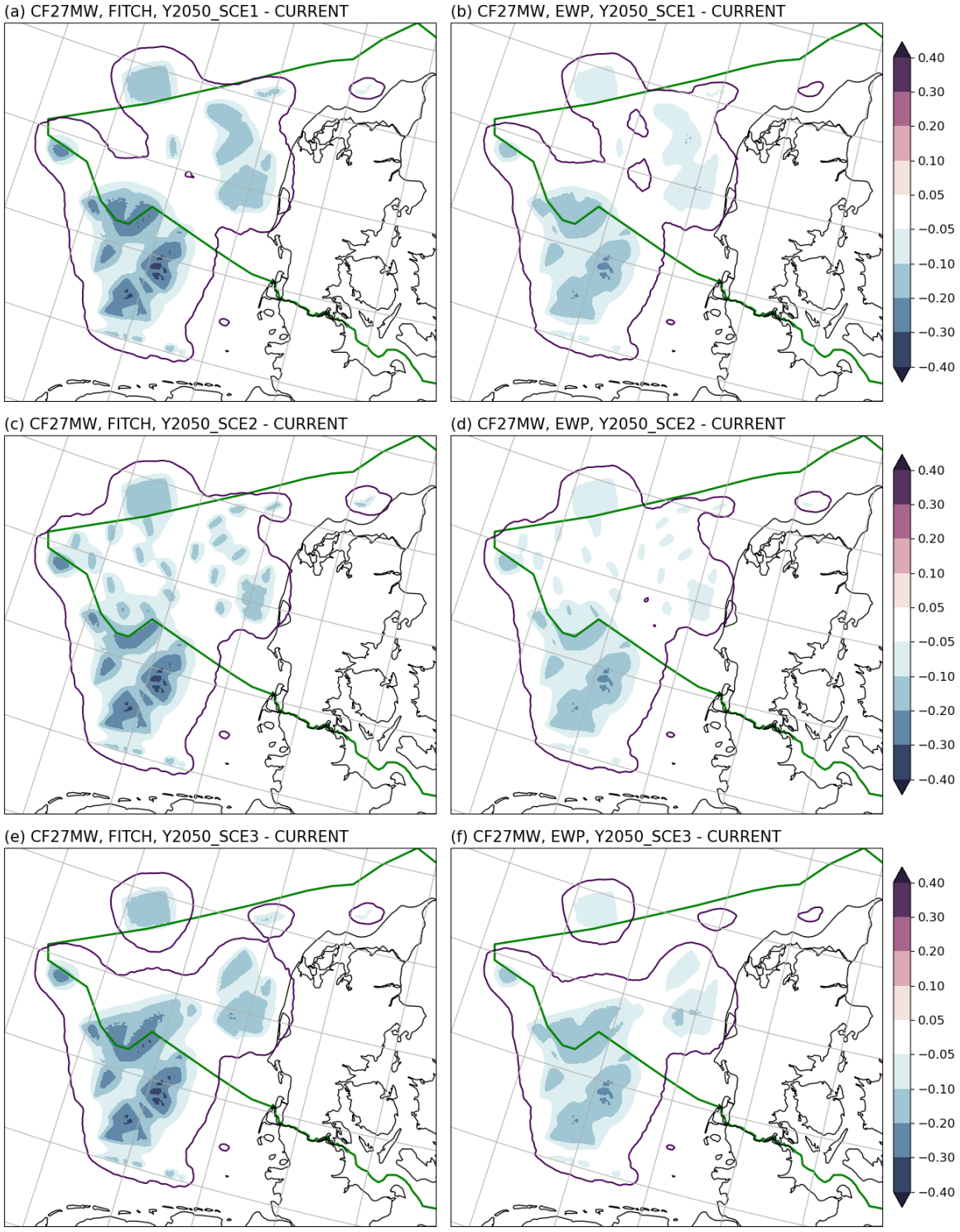


Figure 15: Difference in mean capacity factor [-] from the CURRENT wind farm scenario for all 2022 for the hypothetical 27 MW wind turbine for the three Y2050 scenarios for the FITCH (a, c, e) and EWP (b, d, f) WFPs. The purple line on each figure shows the wake recovery at 98 % from the CURRENT scenario.

Power calculations and wake losses

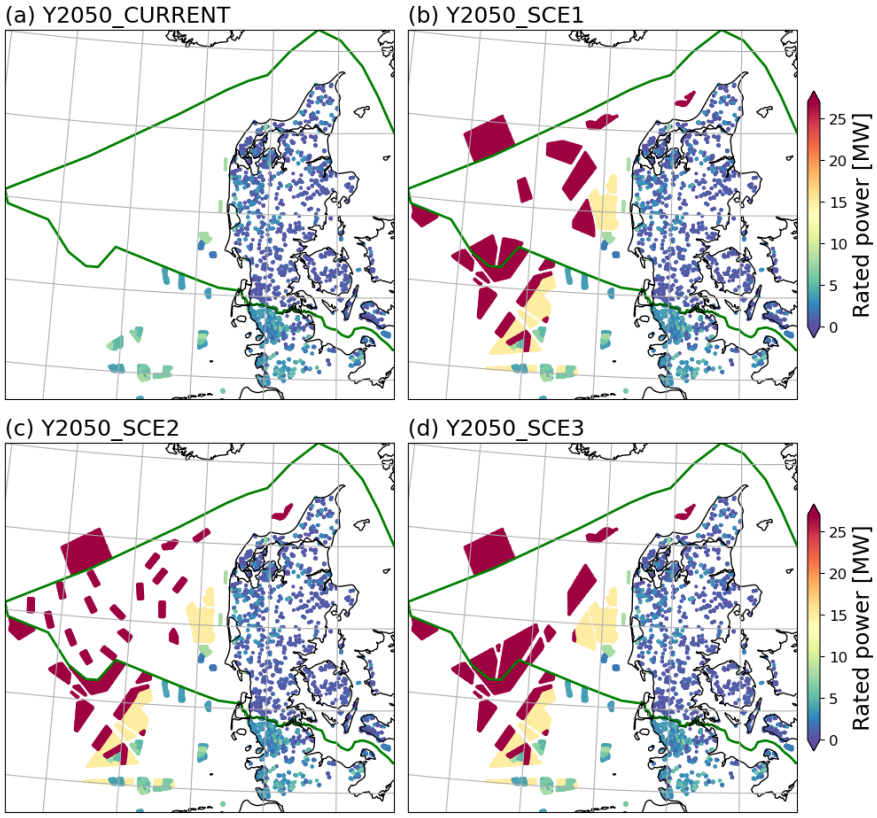


Figure 16: Rated power [MW] of the wind turbines used in the three scenarios: (a) Y2050_CURRENT, (b) Y2050_SCE1, (c) Y2050_SCE2 and (d) Y2050_SCE3 used in the estimation of power quantities. Yellow markers are for the Y2030 scenario (15 MW) and dark red for the Y2050 scenario (27 MW). Other colours represent turbines on land and the CURRENT scenario. Note that the Y2030 does not perfectly match that used in the Large domain.

Table 5 summarises the 2022 annual power values for the Danish North Sea wind farms, estimated from simulations using three Y2050 wind farm scenarios, shown in Figure 16. For comparison, we include the value for the Large domain averaged over the same area for 2019. The average full-load hours across all simulations are very close, ranging from 4142 to 4910, with slightly lower values in the Fitch simulations than in the EWP simulations. The Y2050_SCE2 scenario has the highest FLH values. These values for the Large domain for 2019 are within the range of those computed for the Small Danish domain, but slightly larger than Y2050_SCE1, which has a similar wind farm layout.

The differences between the scenarios can be explained by the spatial patterns in FLH and wake losses in Figure 17. The small compact wind farms in the Y2050_SCE2 suffer from fewer internal wakes than the larger wind farms in the other two scenarios. One or two of the Y2050_SCE2 wind farms are affected by the wake of the Norwegian wind farms, but the effect is compensated for by many wind farms in the north, where wind resources are plentiful. Within the wind farms in the Danish EEZ, in these scenarios, wakes are dominated by internal wakes, except for the large cluster of wind farms near the coast, where there are some farm-to-farm wake effects. This effect is also minimised in the Y2050_SCE2 wind farm scenario, which is the most efficient of the three. Still, it will likely be more expensive to install due to the cost of long-distance cabling and other factors.

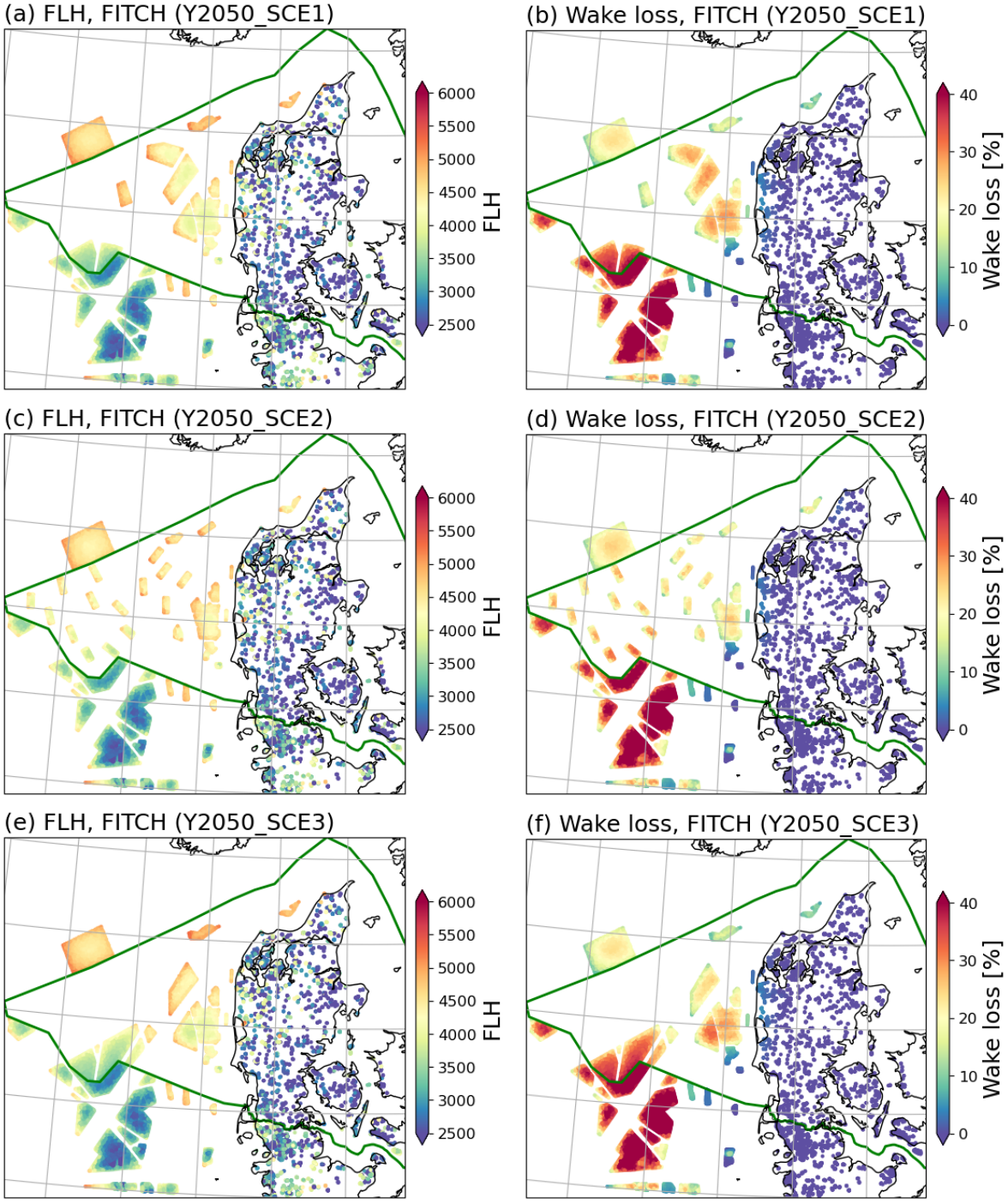


Figure 17: Annual FLHs [h] (left) and wake losses [%] (right) per wind turbine in the three Y2050 wind farm scenarios for 2022 using the Fitch WFP.

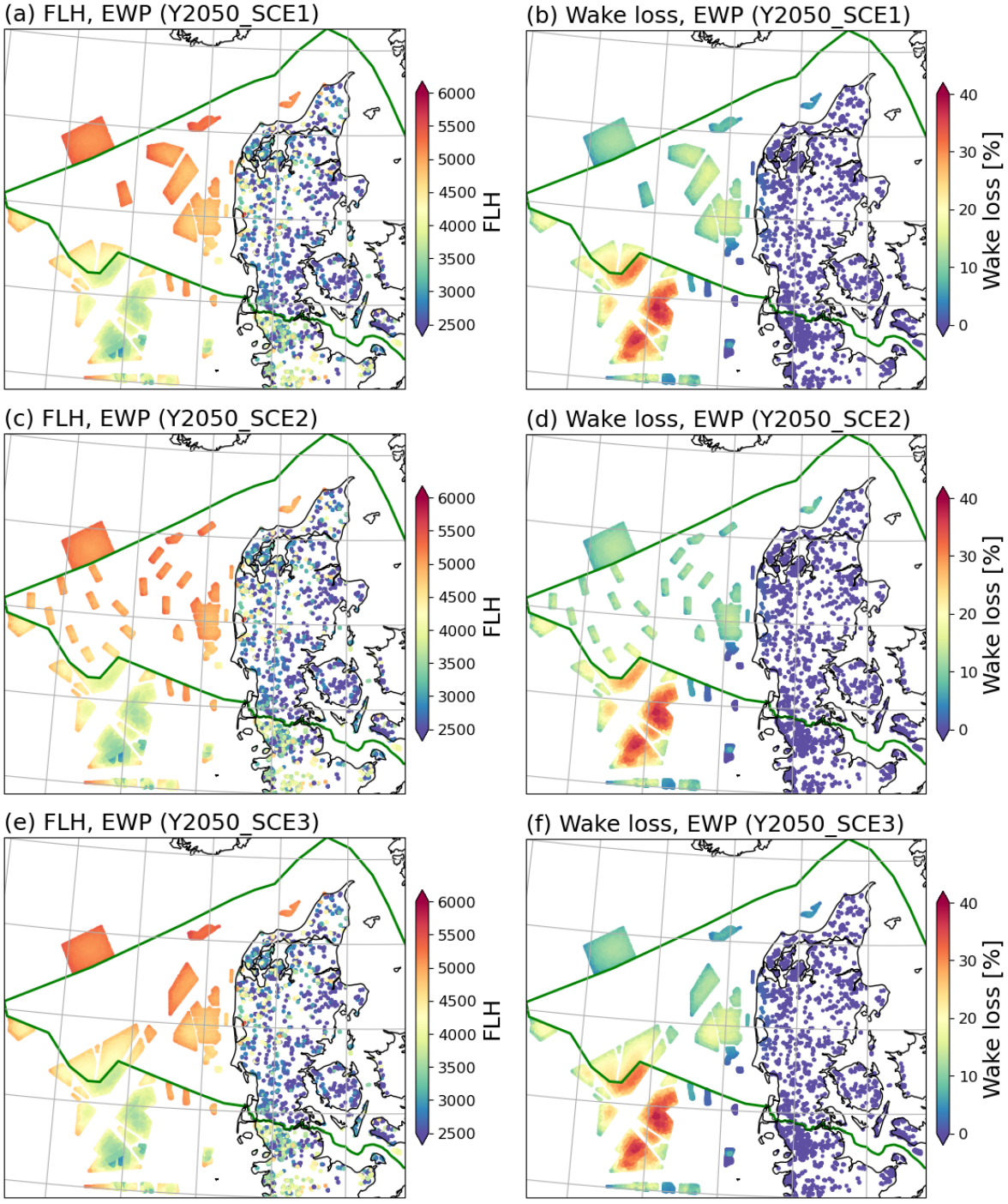


Figure 18: Annual FLHs [h] (left) and wake losses [%] (right) per wind turbine in the three Y2050 wind farm scenarios for 2022 using the EWP WFP.

Table 5: Annual mean full load hours, total power yield [TW h], mean capacity factor [%], and mean wake losses [%] relative to the CURRENT scenario of all Danish turbines in the North Sea (west of 8.1 °E) across the three simulated 2050 wind farm scenarios for 2022. We include the corresponding values for the Large domain for 2019 for the same area as "Y2050 (2019)". These values do not account for additional losses due to turbine availability, electrical efficiency, performance, environmental factors, or curtailments.

Wind farm scenario	IC [GW]	WFP	FLH	AEP [TW h]	CF [%]	Wake loss [%]
Y2050_SCE1	35.5	Fitch	4201	145.7	48.0	24.6
Y2050_SCE2	35.3	Fitch	4357	147.4	49.7	21.8
Y2050_SCE3	35.0	Fitch	4142	141.0	47.3	25.5
Y2050 (2019)	34.7	Fitch	4231	146.0	48.3	24.7
Y2050_SCE1	35.5	EWP	4782	166.8	54.6	13.8
Y2050_SCE2	35.3	EWP	4910	167.3	56.0	11.5
Y2050_SCE3	35.0	EWP	4714	161.3	53.8	15.0
Y2050 (2019)	34.7	EWP	4819	167.7	55.0	14.1

4.3 Comparison of the Large and Small Danish domains

Finally, we compare the results from the Large and Small Danish domains for the CURRENT and 2050 scenarios. The simulations and scenarios are not directly comparable for two reasons. First, the scenarios are not identical (compare Figure 5 and Figure 11). Still, the two closest are the Y2050 scenario in the Large domain and the Y2050_SCE1 scenario in the Small Danish domain. Second, we simulated two different years for the two sets of simulations: 2019 in the Large domain and 2022 in the Small Danish domain. As shown in Figure 4 of the interannual variability report [14], the mean wind speeds in 2019 are slightly lower than in 2022 in the northern part of the Danish EZZ, contributing towards slightly higher wake effects.

To further quantify the extent of differences between the two sets of simulations, we show transects of annual mean wind speed at 175 m and 27 MW CF (Figure 19) along 56.8 °N. This transect, shown in Figure 5, cuts through regions with similar installed-capacity densities in the Large domain Y2050 and the Small Danish domain Y2050_SCE1 simulations. The transect also shows the intersected capacity density, which seems higher in the Small Danish domain. However, this perception is misleading, as it arises from the need to distribute the same installed capacity density across WRF model grid squares of different area (3 km x 3 km vs 1.5 km x 1.5 km). Along the transect (Figure 19a), mean wind speeds in the CURRENT simulations are larger by about 0.3 m s^{-1} in the Small Danish domain simulations for 2022 than in the Large domain simulations for 2019. This is partly due to interannual variability (winds in 2022 are higher than in 2019 in this area, see Figure 19a) and to the low-resolution representation of the Norwegian mountains in the Small Danish domain simulations, which affects the magnitude of the wind speed. Wind speed deficits are comparable between the two simulations for the Norwegian wind farm, with similar installed capacity density. As the flow approaches the coast, the differences nearly disappear.

Figure 6 and Figure 14(a,b) show the mean differences in yearly mean wind speed and capacity factor for a 27 MW wind turbine between the CURRENT and 2050 scenarios for each simulation domain. The differences in 175 m wind speed show small variations between each other, but the overall extent and magnitude of the changes are comparable. Analogously, Figure 7(c and d) and Figure 15(a,b), which show the changes in the capacity factor for a 27 MW wind turbine, show similar differences in the shape and magnitude in the Danish EEZ. Near the German wind farms, differences are larger in the Large domain simulations than in the Small Danish simulations, again due to differences in installed capacity. Despite these differences, the location of the line of wake recovery at the 98 % from the CURRENT scenario is nearly identical between the two sets of simulations.

Table 5 shows very similar estimates of the wake losses between the Y2050 scenario in the Large

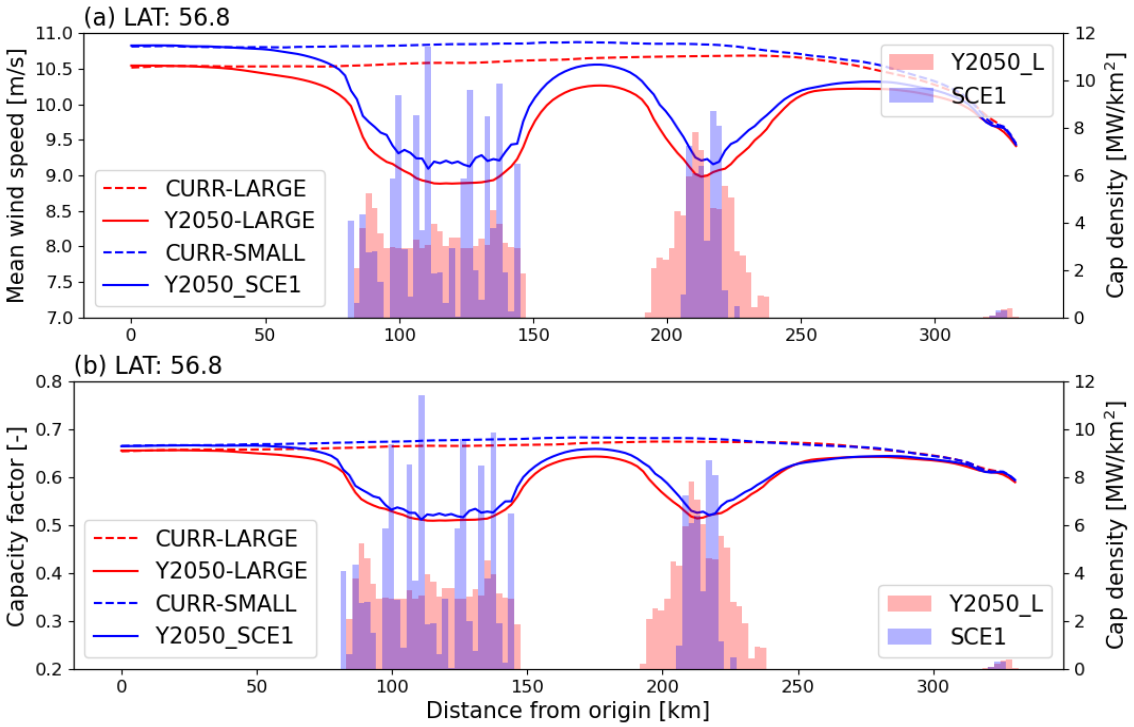


Figure 19: Comparing the (a) mean wind speed [m s^{-1}] and the (b) 27 MW turbine CF [-] along a transect (Figure 5) at 56.8 °N for the Large domain Y2050 (2019) and the Small Danish domain Y2050_SCE1 (2022) wind farm scenarios. The red and blue-coloured boxes show the installed capacity density per intersected WRF model grid box in these scenarios, with the scale on the right. Note that the y-axis starts at a wind speed of 7 m s^{-1} and a capacity factor of 0.2.

domain and Y2050_SCE1 in the Small Danish domain. In the Fitch-driven simulations, the wake losses are 24.6 % and 24.7 %, respectively; and in the EWP simulations 13.8 % and 14.1 %, respectively. These differences align with the higher wind speeds in 2022 compared to 2019, the slightly smaller installed capacity in the Y2050 scenario, and the fact that large WRF model grid cells tend to produce smaller wake losses than smaller ones for the same area [12].

5 Summary and conclusions

The operation of extensive offshore wind farms or clusters of wind farms leads to a marked decrease in wind speed, potentially reaching levels between 1 m s^{-1} to 3 m s^{-1} outside the wind farm area. This effect can extend from 20 km to 80 km downstream, based on simulations from this and the previous study [15]. This phenomenon is known as the large-scale wind farm wake.

Previously, we analysed 2019 atmospheric flow simulations to estimate wind resources in the North Sea, the South Baltic Sea, and the Kattegat [13]. We considered three scenarios: no wind farms, current wind farm installations as of November 2021, and projected wind farm deployment in 2030. In this report, we extend the simulations to include a 2050 wind farm expansion scenario, adding about 30 GW of new offshore wind capacity in the Danish North Sea EEZ.

We conducted two new sets of mesoscale simulations for the 2050 scenarios, using the same overall WRF model configuration but with different domain locations and grid spacings. The first set is designed to be compared with previous simulations for the CURRENT and Y2030 scenarios [13, 14] and to explore the influence of the Y2050 wind farm scenario on atmospheric flow, wakes, and Danish power output. The second set utilises a smaller domain covering the Danish North Sea at a higher resolution, with three different wind farm configurations, each with identical installed capacity. The second set aims to identify an optimal distribution of wind farms across the Danish North Sea with the same total capacity, primarily to reduce power losses due to wake effects. An additional goal was to assess the impact of WRF model resolution on wake behaviour and recovery distances for similar wind farm configurations.

- The mesoscale model simulations assume that future turbines in 2050 will have a capacity of 27 MW, a hub height of 180 m, and a rotor diameter of 300 m. In these scenarios, the installed offshore capacity in Danish waters increases from 2.3 GW in 2021 to 47.4 GW in 2050.
- Large offshore wind farms reduce wind speeds within and downwind of clusters. In the 2050 scenario, the Danish EEZ in the North Sea experiences wind speed deficits of up to −2.5 m s^{-1} within large wind farms near the German border. Half the area of the Danish North Sea EEZ has mean wind speed reductions of at least −0.25 m s^{-1}.
- The simulations show minor changes in surface temperature (about 0.07 °C degrees offshore), an increase in boundary layer height of 40–80 m, and slight changes in cloud fraction (4%), mostly near large clusters. These changes are likely not statistically significant at the 95 % level but are robust under some atmospheric conditions.
- The 2050 offshore wind scenarios show wake losses of 14–25%, only slightly higher than in the 2030 scenario (11–21%), due to larger installed capacity and wind farm clustering. The small increase in wake losses from 2030 to 2050 is due to low installed capacity densities and the location of future wind farms in areas with excellent wind resources.
- Despite considerable wake losses, annual energy production increases significantly in future scenarios due to higher installed capacity and the placement of offshore wind farms in areas with abundant wind resources. For Denmark, the wind turbines in the simulation under the CURRENT scenario have a power yield of ∼24 TWh, which increases to 84–94 TWh in the 2030 scenario and 204–232 TWh in the 2050 scenario, depending on the WFP used.
- Among the three tested wind farm scenarios, the one featuring many small, densely packed farms offers the optimal balance between minimising wake effects and maximising energy output. However, it may entail higher infrastructure costs. This distributed configuration reduces internal wakes by using smaller areas and placing them in regions with stronger winds. The other two scenarios exhibit only minor differences in energy production and full load hours.
- With ample space and excellent wind conditions, many scenarios can achieve 35 GW of offshore wind capacity in the Danish North Sea, maximising power output. The results of the various scenarios show that both large, low-capacity-density farms and smaller farms help reduce wake effects, making either option feasible.

References

[1] Karim Ali, David M. Schultz, Alistair Revell, Timothy Stallard, and Pablo Ouro. Assessment of five wind-farm parameterizations in the Weather Research and Forecasting Model: A case study of wind farms in the North Sea. *Monthly Weather Review*, 151(9):2333–2359, August 2023.

[2] Nicola Bodini, Simon Castagneri, and Mike Optis. Long-term uncertainty quantification in WRF-modeled offshore wind resource off the US Atlantic coast. *Wind Energy Science*, 8(4):607–620, April 2023.

[3] Nicola Bodini, Mike Optis, Stephanie Redfern, David Rosencrans, Alex Rybchuk, Julie K. Lundquist, Vincent Pronk, Simon Castagneri, Avi Purkayastha, Caroline Draxl, Raghavendra Krishnamurthy, Ethan Young, Billy Roberts, Evan Rosenlieb, and Walter Musial. The 2023 National Offshore Wind data set (NOW-23). *Earth Syst. Sci. Data*, pages 1–57, 2023.

[4] Neil N. Davis, Jake Badger, Andrea N. Hahmann, Brian O. Hansen, Niels G. Mortensen, Mark Kelly, Xiaoli G. Larsén, Bjarke T. Olsen, Rogier Floors, Gil Lizcano, Pau Casso, Oriol Lacave, Albert Bosch, Ides Bauwens, Oliver James Knight, Albertine Potter van Loon, Rachel Fox, Tigran Parvanyan, Søren Bo Krohn Hansen, Duncan Heathfield, Marko Onninen, and Ray Drummond. The Global Wind Atlas: A high-resolution dataset of climatologies and associated web-based application. *Bulletin of the American Meteorological Society*, 104(8):E1507–E1525, 2023.

[5] M. Dirksen, Ine Wijnant, A.P. Siebesma, Peter Baas, and Natalie E. Theeuwes. Validation of wind farm parameterisation in weather forecast model harmonie-arome: Analysis of 2019. Technical report, Delft University of Technology, Netherlands, 2022.

[6] Martin Dörenkämper, Bjarke T Olsen, Björn Witha, Andrea N Hahmann, Neil N Davis, Jordi Barcons, Yasemin Ezber, Elena García-Bustamante, J Fidel González-Rouco, Jorge Navarro, et al. The making of the New European Wind Atlas –part 2: Production and evaluation. *Geoscientific Model Development*, 13(10):5079–5102, 2020.

[7] Energistyrelsen. Notat om scenarier for havvindudbygning frem mod 2050. Technical report, ENS, 2024.

[8] Jana Fischereit, Roy Brown, Xiaoli Guo Larsén, Jake Badger, and Graham Hawkes. Review of mesoscale wind-farm parametrizations and their applications. *Boundary-Layer Meteorology*, 182(2):175–224, February 2022.

[9] Anna C Fitch, Joseph B Olson, Julie K Lundquist, Jimy Dudhia, Alok K Gupta, John Michalakes, and Idar Barstad. Local and mesoscale impacts of wind farms as parameterized in a mesoscale NWP model. *Mon. Wea. Rev.*, 140(9):3017–3038, September 2012.

[10] O. García-Santiago, J. Badger, A. N. Hahmann, P. J. H. Volker, S. Ott, M. P. van der Laan, and M. Kelly. A wind-farm wake-turbulence parameterization for the WRF model (ewp v2.0). *EGUsphere*, 2026:1–34, 2026.

[11] Oscar García-Santiago, Andrea N. Hahmann, Jake Badger, and Alfredo Peña. Evaluation of wind farm parameterizations in the WRF model under different atmospheric stability conditions with high-resolution wake simulations. *Wind Energy Sci.*, 9:963–979, 2024.

[12] Oscar M. Garcia-Santiago, M. Paul van der Laan, Alfredo Peña, and Jake Badger. Impact of grid resolution in subgrid-scale wind farm parametrizations of mesoscale models and the need for thrust-coefficient calibration. In *The Science of Making Torque from Wind 2026 (TORQUE 2026)*, Journal of Physics: Conference Series. IOP Publishing, 2022.

[13] Andrea N. Hahmann, Marc Imberger, Jana Fischereit, Nicolas G. Alonso de Linaje, and Jake Badger. Environmental mapping and screening of the offshore wind potential in Denmark: Comparison of old and new simulations. Technical report, DTU Wind, 2025. https://orbit.dtu.dk/files/422587231/ENSreport_Updated_v2.0_Final.pdf.

[14] Andrea N. Hahmann, Marc Imberger, Jana Fischereit, Nicolas G. Alonso de Linaje, and Jake Badger. Environmental mapping and screening of the offshore wind potential in Denmark: Interannual variability. Technical report, DTU Wind, 2025. https://orbit.dtu.dk/files/422587458/ENSreport_Interannual_Variability_Final.pdf.

[15] Andrea N. Hahmann, Marc Imberger, Jana Fischereit, Nicolas G. Alonso de Linaje, and Jake Badger. Environmental mapping and screening of the offshore wind potential in Denmark. sensitivity mapping: Wind. Technical Report Report Number DTU E-0255, DTU Wind, 2025. https://orbit.dtu.dk/files/400503926/ENSreport_V4.0_1May2025.pdf.

[16] Bjarke T. Olsen, Andrea N. Hahmann, Anna Maria Sempreviva, Jake Badger, and Hans E. Jørgensen. An intercomparison of mesoscale models at simple sites for wind energy applications. *Wind Energy Science*, 2(1):211–228, May 2017.

[17] S C Pryor, T J Shepherd, P J H Volker, A N Hahmann, and R J Barthelmie. "Wind Theft" from onshore wind turbine arrays: Sensitivity to wind farm parameterization and resolution. *Journal of Applied Meteorology and Climatology*, 59(1):153–174, 2020.

[18] Balthazar M Sengers, Lukas Vollmer, and Martin Dörenkämper. Beyond standard Fitch: Validating WRF's wind farm parametrizations with offshore scada data. In *Wind Energy Science Conference, Nantes, France, 6/25/2025*, 2025.

[19] Tristan J. Shepherd, R. J. Barthelmie, and S. C. Pryor. Sensitivity of wind turbine array downstream effects to the parameterization used in WRF. *Journal of Applied Meteorology and Climatology*, 59(3):333–361, 2020.

[20] C. Skamarock, B. Klemp, Jimy Dudhia, O. Gill, Zhiquan Liu, Judith Berner, Wei Wang, G. Powers, G. Duda, Dale Barker, and Xiang-yu Huang. A Description of the Advanced Research WRF Model Version 4.2. Technical Report NCAR/TN-556+STR), NCAR/UCAR, 2021.

[21] Patrick J. H. Volker, Jake Badger, Andrea N. Hahmann, and S. Ott. The explicit wake parametrisation V1.0: A wind farm parametrisation in the mesoscale model WRF. *Geoscientific Model Development*, 8(11):3715–3731, 2015.

[22] Patrick J. H. Volker, Andrea N. Hahmann, Jake Badger, and Hans E Jørgensen. Prospects for generating electricity by large onshore and offshore wind farms. *Environ. Res. Lett.*, 12:034022, 2017.

[23] DTU Wind. PyWake. https://gitlab.windenergy.dtu.dk/TOPFARM/PyWake.

ANNEXES

Annex 1 Analysis for the whole domain

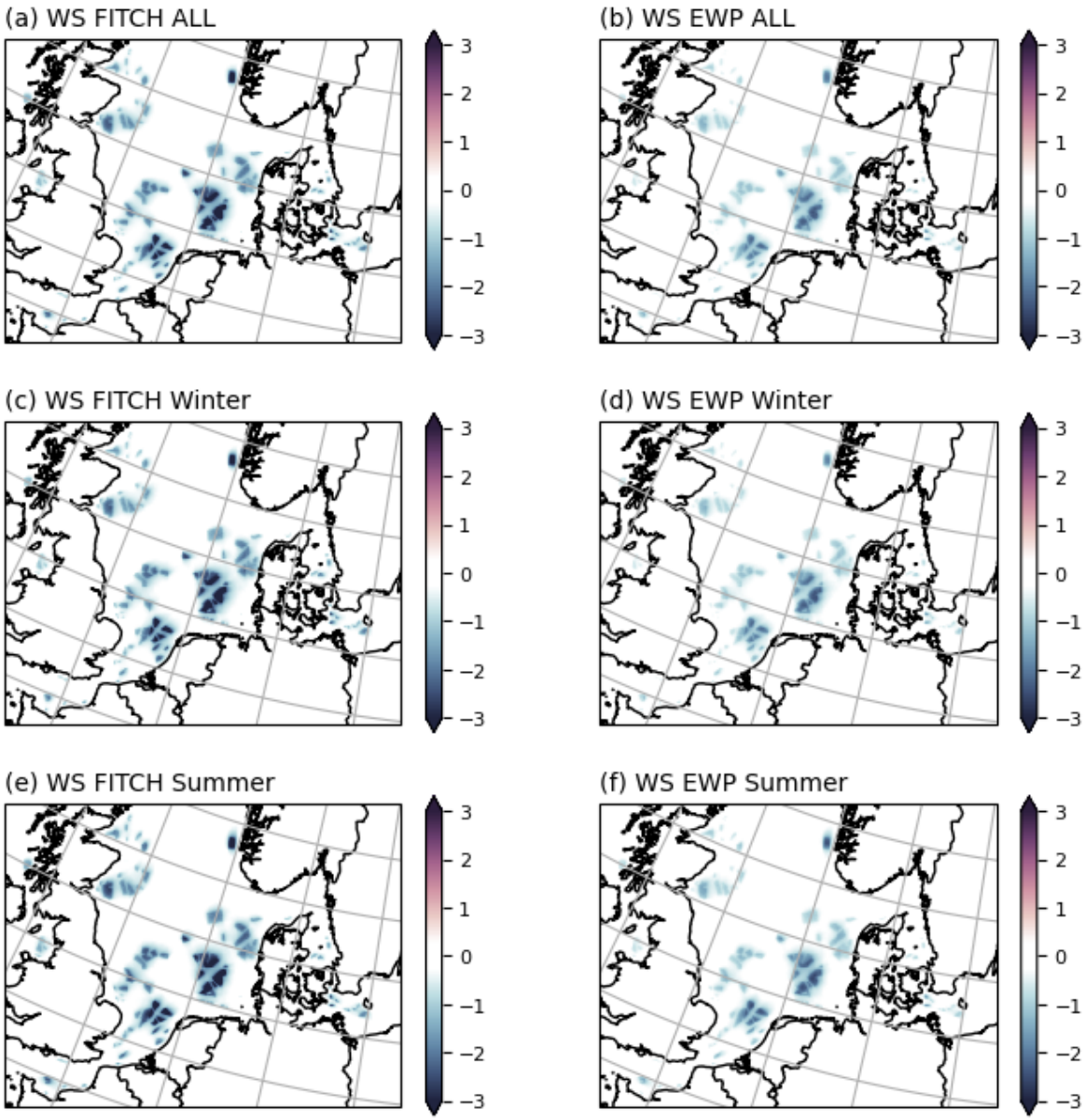


Figure 20: Mean wind speed differences [m s^{-1}] at 150 m between the Large domain Y2050 and CURRENT scenario for the FITCH (a, c, and e) and the EWP (b,d, f) WFPs.

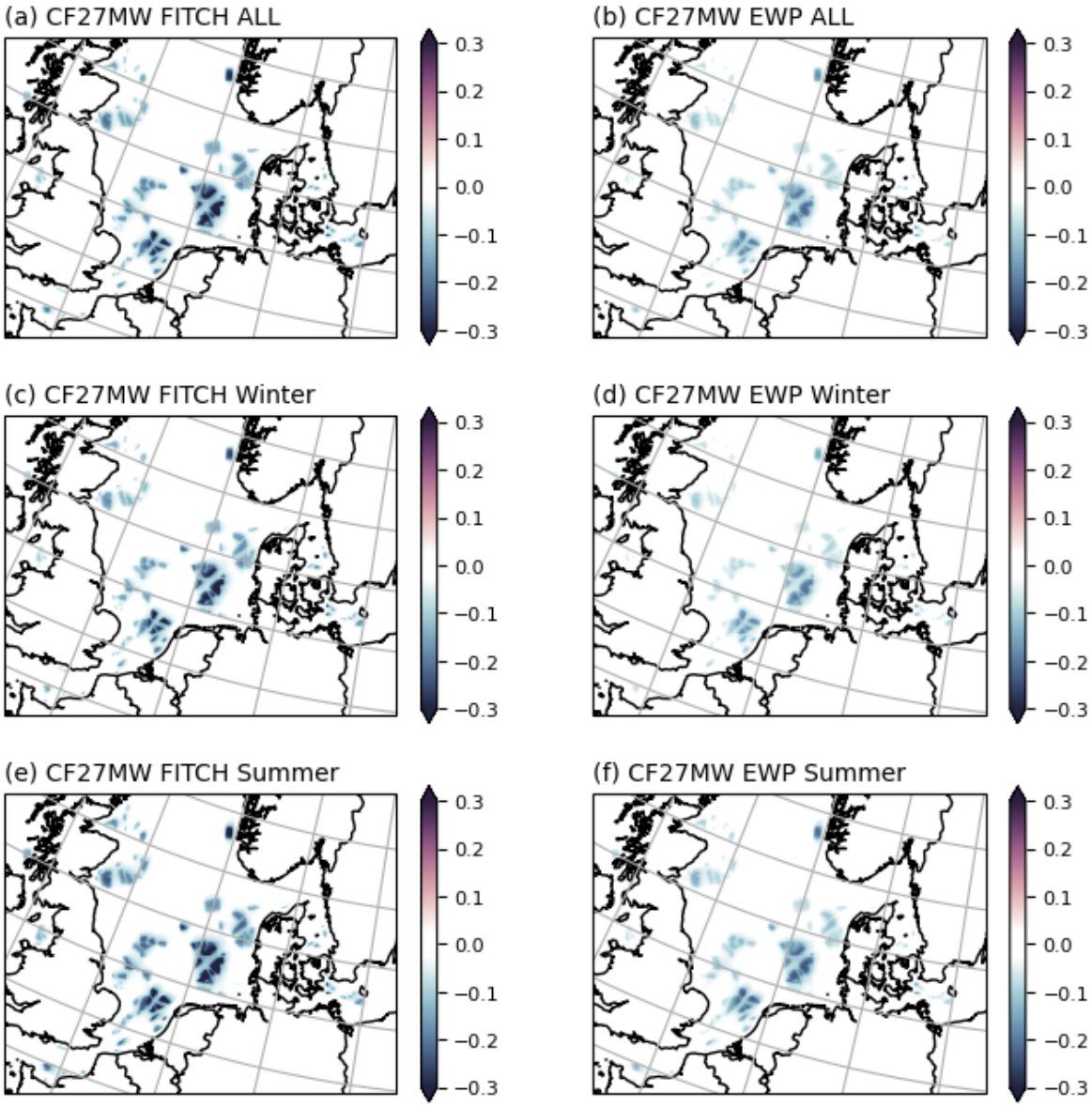


Figure 21: Mean capacity factor differences [-] for the hypothetical 27 MW wind turbine between the Large domain Y2050 and CURRENT scenario for the FITCH (a, c, and e) and the EWP (b,d, f) WFPs.

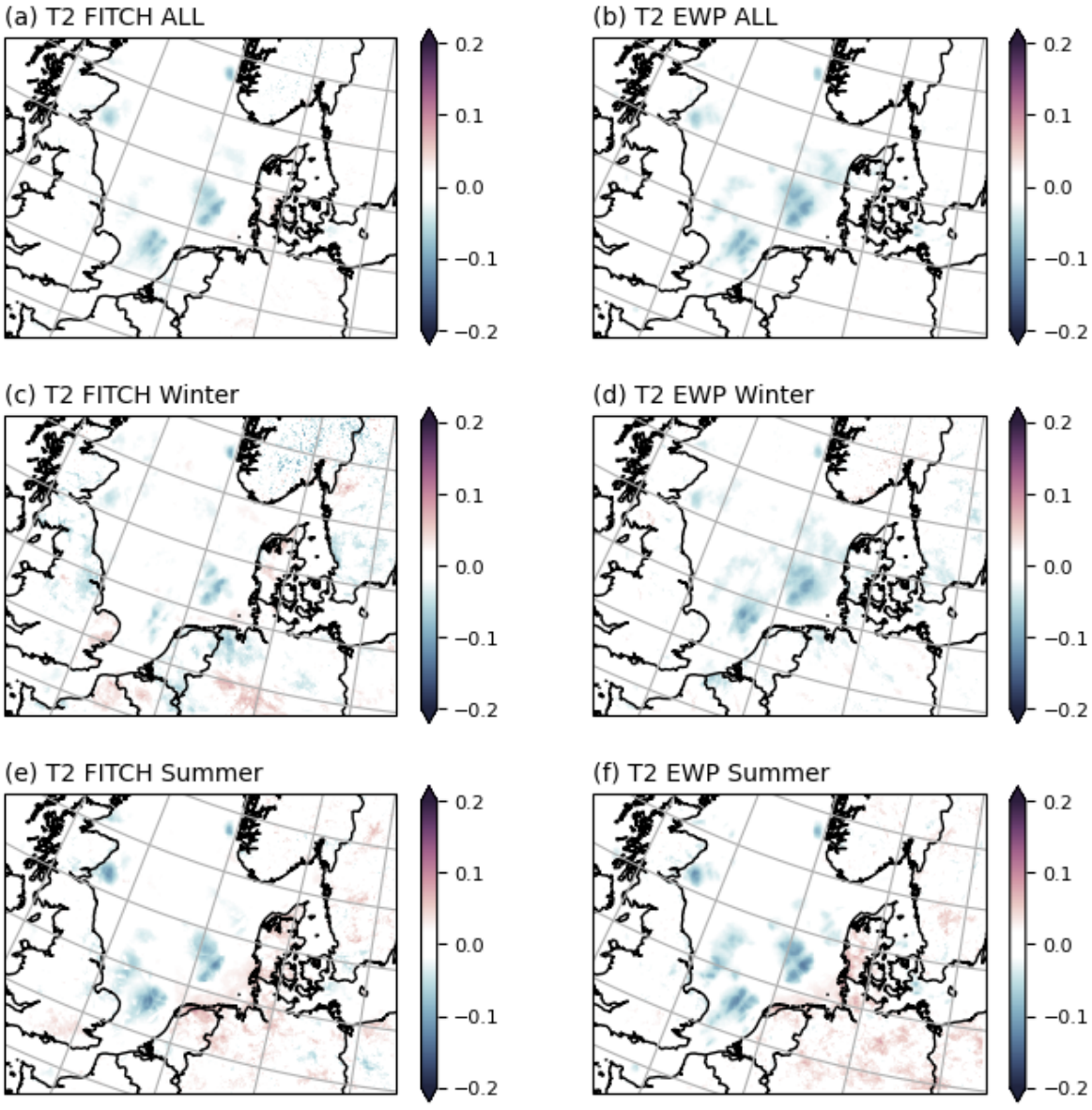


Figure 22: Mean 2-m temperature differences [°C] between the Large domain Y2050 and CURRENT scenario for the FITCH (a, c, and e) and the EWP (b,d, f) WFPs.

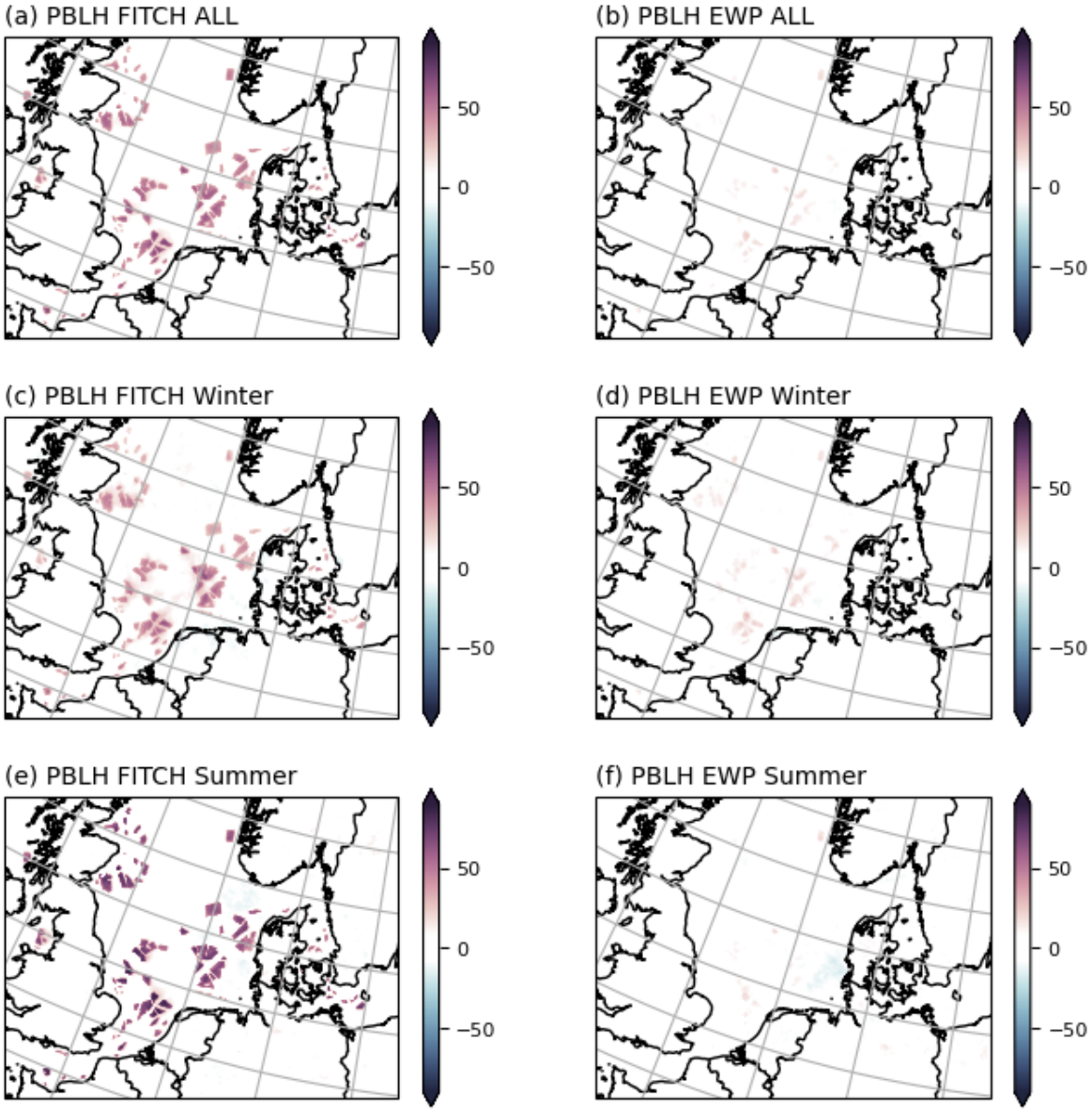


Figure 23: Mean boundary layer differences [m] between the Large domain Y2050 and CURRENT scenario for the FITCH (a, c, and e) and the EWP (b,d, f) WFPs.

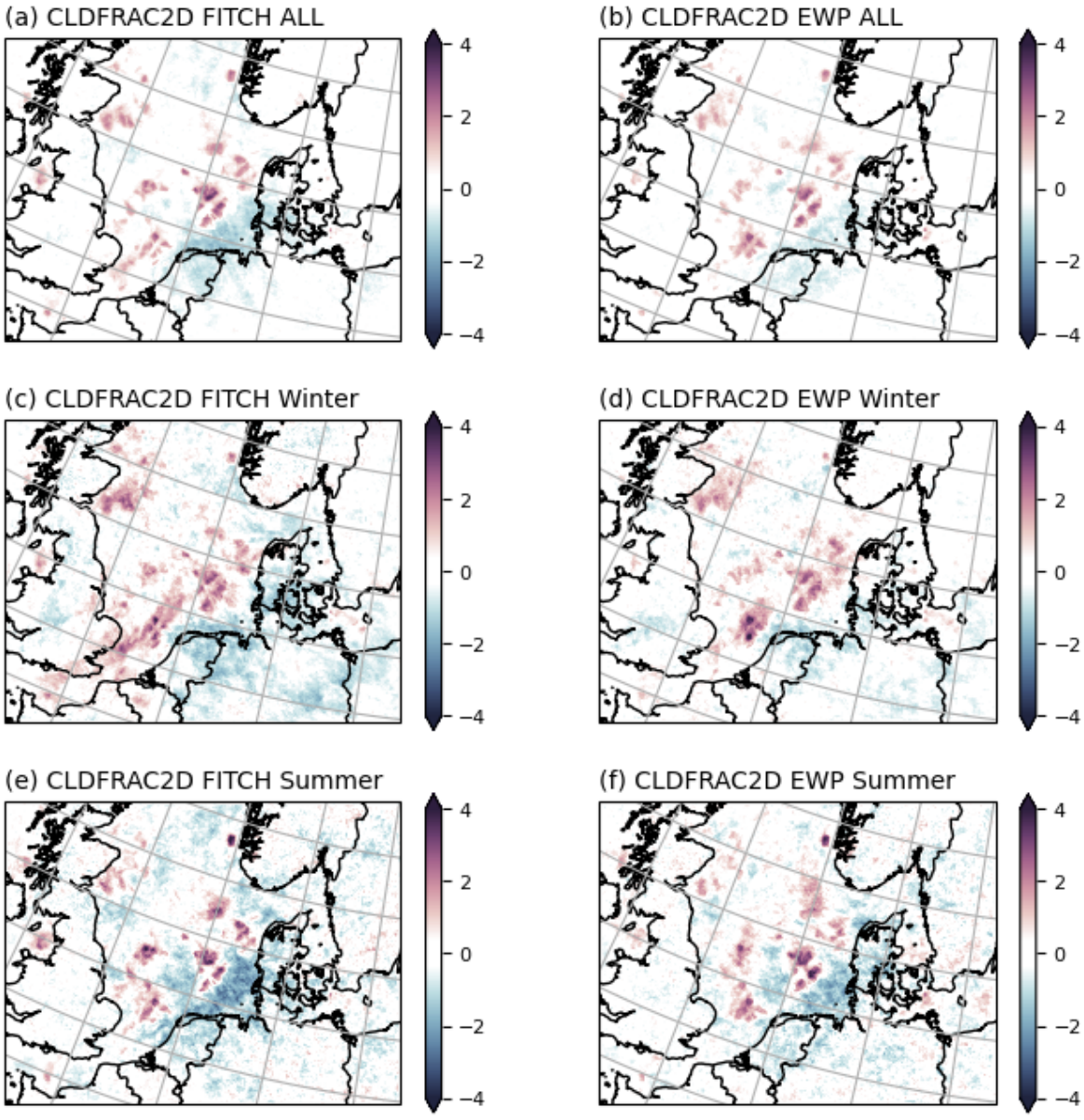


Figure 24: Mean cloud fraction differences [%] between the Large domain Y2050 and CURRENT scenario for the FITCH (a, c, and e) and the EWP (b,d, f) WFPs.